COMPARATIVE STUDY OF THE SOLUBILITY OF DMF IN SILICONE OIL FOR USE IN A DROPLET-BASED MICROFLUIDIC SYSTEM TOWARDS SYNTHESIS OF MOF NANOPARTICLES

DAMLACIK BAZLI MİKROAKIŞKAN SİSTEMDE MOF NANOPARTİKÜLLERİNİN SENTEZİNE YÖNELİK KULLANIMI İÇİN SİLİKON YAĞINDA DMF ÇÖZÜNÜRLÜĞÜNÜN KARŞILAŞTIRILMALI ÇALIŞMASI

GAYE KORKMAZ

ASSOC. PROF. DR. SELİS ÖNEL KAYRAN

Supervisor

Submitted to

Graduate School of Science and Engineering of Hacettepe University

as a Partial Fulfillment to the Requirements

for the Award of the Degree of Master of Science

in Chemical Engineering

September 2023

ABSTRACT

COMPARATIVE STUDY OF THE SOLUBILITY OF DMF IN SILICONE OIL FOR USE IN A DROPLET-BASED MICROFLUIDIC SYSTEM TOWARDS SYNTHESIS OF MOF NANOPARTICLES

Gaye Korkmaz

Master of Science , Chemical Engineering

Supervisor: Assoc. Prof. Dr. Selis Önel Kayran

September 2023, 74 pages

Synthesis of nanoparticles with enhanced adsorption capacities based on a complex metal organic framework (MOF) structure requires the employment of supersaturated solutions prepared with solvents that possess multiple properties at elevated temperatures. N,n-dimethylformamide (DMF), represented as $HCON(CH_3)_2$, is the widely used solvent with a high solvating and coordinating ability for metal salts and organic ligands, thermal stability at high temperatures, and high dispersing capacity in the synthesis of nanoparticles with MOF structures. Synthesis of MOF particles is usually performed using hydrothermal and/or solvothermal methods at high temperatures in conventional batch reactors using conventional heating systems. Single- or two-phase microfluidic systems that enable the use of smaller amounts of solution or microwave systems that provide rapid heating of the solution as it flows have become promising methods yielding more uniform smaller particles and reduced synthesis times. Solubility of the solvent is a critical factor when the solution is used in two-phase suspensions or two-phase microfluidic systems involving an oil as the carrier phase. Silicone oil (Polydimethylsiloxane, $[-Si(CH^3)^2O-]^n)]$ is a nonpolar hydrophobic substance that is almost immiscible with DMF and is frequently used as the

carrier fluid in two-phase droplet microfluidics. The promotion of the dissolution of the solvent into the carrier oil phase due to surface tension or convective forces in suspended systems, which is further enhanced in flowing systems and at the micro scale, creates a serious problem. Any mass transfer that may occur between the droplet phase and the continuous phase changes the concentration of the precursor solution in the droplets and, accordingly, the quality of the final product. This is an undesirable situation that must be managed by preventing the mass transfer between the two phases or by compensating for the possible mass loss in the initial precursor solution. In this thesis, we conducted a comparative study to investigate the solubility of DMF in silicon oils with different viscosities, 100 cSt, 500 cSt, and 1000 cSt, at both micro and macro scales with and without flow effects at various temperatures, 25 °C, 50 °C, 75 °C, and 100 °C. Any possible diffusion between the two phases can affect the synthesis time and the quality of the final products in two-phase microfluidic systems, where suspended uniform droplets flowing with the oil phase are used as picoliter vessels. Such a problem has not been pronounced until now in the studies of MOF syntheses employing microfluidic systems, where DMF and silicone oil are used together, because the microfluidic channels consisted of opaque capillary tubes. Such systems do not allow for the observation of the whole process starting from the formation of the droplets to the formation of particles on an optical microscope. The transparent microfluidic devices used in this study allowed for the observation of the shrinkage of droplets on an inverted microscope. To identify the effects of the droplet-based microfluidic system on the mass transport into the oil, we compared the solubility of DMF in silicone oil at macro and micro scales and under stationary and flow conditions using three different systems: 1. A stationary macro-scale system, 2. a stationary micro-scale system, and 3. a microfluidic system. We discussed the effects of size and convective mass diffusion by comparing the results obtained at the macro and micro scales using stationary and flow conditions and showed that solubility is enhanced under flow conditions at smaller scales.

Keywords: Two phase microfluidics, Solubility, N,n-dimethylformamide (DMF), Polydimethylsiloxane (PDMS), Silicone oil, Mass transport, Diffusion, Convection, Metal organic framework (MOF)

ÖZET

DAMLACIK BAZLI MİKROAKIŞKAN SİSTEMDE MOF NANOPARTİKÜLLERİNİN SENTEZİNE YÖNELİK KULLANIM İÇİN SİLİKON YAĞINDA DMF ÇÖZÜNÜRLÜĞÜNÜN KARŞILAŞTIRILMALI ÇALIŞMASI

Gaye Korkmaz

Yüksek Lisans, Kimya Mühendisliği

Danışman: Assoc. Prof. Dr. Selis Önel Kayran

Eylül 2023, 74 sayfa

Metal organik çerçeve (MOF) yapısına sahip geliştirilmiş adsorpsiyon kapasitelerine gösteren nanopartiküllerin sentezi, yüksek sıcaklıklarda birden fazla özelliğe sahip solventlerle hazırlanan aşırı doymuş çözeltilerin kullanılmasını gerektirir. N,n-dimetilformamid (DMF), metal tuzları ve organik ligandlar için yüksek çözme yeteneğine sahiptir, ve yüksek sıcaklıklarda termal stabilitesi yüksektir. Bu özellikleri sebebiyle MOF yapısına sahip nanopartiküllerin sentezinde yaygın olarak kullanılan bir çözücüdür. MOF parçacıklarının sentezi genellikle geleneksel ısıtma sistemlerini kullanan geleneksel kesikli reaktörlerde, yüksek sıcaklıklarda hidrotermal ve/veya solvotermal yöntemler kullanılarak gerçekleştirilir. Daha küçük miktarlarda çözeltinin kullanılmasını sağlayan tek veya iki fazlı mikroakışkan sistemler veya çözeltinin aktıkça hızla ısıtılmasını sağlayan mikrodalga sistemleri, daha düzgün daha küçük parçacıklar sağlayan ve sentez sürelerini azaltan umut verici yöntemler haline gelmiştir. Çözeltinin iki fazlı süspansiyonlarda veya taşıyıcı faz olarak bir yağın kullanıldığı iki fazlı mikroakışkan sistemlerde kullanıldığı durumlarda solventin çözünürlüğü kritik bir faktördür. Silikon

yağı (Polidimetilsiloksan), DMF ile hemen hemen karışmayan, polar olmayan hidrofobik bir maddedir ve sıklıkla iki fazlı damlacık mikroakışkanlarda taşıyıcı akışkan olarak kullanılır. Süspansiyon sistemlerinde yüzey gerilimi veya konvektif kuvvetler nedeniyle solventin taşıyıcı yağ fazında çözünmesinin teşvik edilmesi, ve akışlı sistemlerde ve mikro ölçekte daha da artması ciddi bir sorun oluşturmaktadır. Damlacık fazı ile sürekli faz arasında meydana gelebilecek herhangi bir kütle transferi, damlacıklardaki öncül çözeltinin konsantrasyonunu ve buna bağlı olarak nihai ürünün kalitesini değiştirir. Bu, iki faz arasındaki kütle aktarımının engellenmesi veya başlangıç öncül çözeltisindeki olası kütle kaybının telafi edilmesi yoluyla yönetilmesi gereken istenmeyen bir durumdur. Bu tezde, DMF'nin farklı viskozitelerdeki (100 cSt, 500 cSt ve 1000 cSt) silikon yağlarındaki çözünürlüğünü hem mikro hem de makro ölçekte, çeşitli sıcaklıklarda, 25 °C, 50°C, 75°C ve 100°C, akış etkisinin olduğu ve olmadığı durumlarda araştırmak için karşılaştırmalı bir çalışma yaptık. İki faz arasındaki olası herhangi bir difüzyon, yağ fazıyla birlikte akan asılı eş boyutlu damlacıkların pikolitre reaktör olarak kullanıldığı iki fazlı mikroakışkan sistemlerde sentez süresini ve nihai ürünlerin kalitesini etkileyebilir. DMF ve silikon yağının bir arada kullanıldığı mikroakışkan sistemlerde gerçekleştirilen MOF sentezi çalışmalarında, mikroakışkan kanalların opak kılcal tüplerden oluşması nedeniyle şu ana kadar böyle bir sorun dile getirilmemiştir. Bu tür sistemler, damlacıkların oluşumundan başlayarak parçacıkların oluşumuna kadar olan tüm sürecin optik mikroskopta gözlemlenmesine olanak sağlamamaktadır. Bu çalışmada kullanılan şeffaf mikroakışkan cihazlar, damlacıkların küçülmesinin mikroskopta gözlemlenmesine olanak sağlamıştır. Damlacık bazlı mikroakışkan sistemin damlacık fazından yağ fazına doğru gerçekleşen kütle transferi üzerindeki etkilerini tanımlamak için, üç farklı sistem kullanarak DMF'nin silikon yağındaki çözünürlüğünü makro ve mikro ölçeklerde ve sabit ve akış koşulları altında karşılaştırdık: 1. Durgun makro ölçekli sistem, 2. durgun mikro ölçekli sistem ve 3. mikroakışkan sistem. Durgun ve akış koşullarını kullanarak makro ve mikro ölçeklerde elde edilen sonuçları karşılaştırdık ve deneysel ortamın ölçeğinin ve konvektif etkilerin kütle transferini nasıl etkilediğini tartıştık. Durgun makro sistemde yapılan deneyler sıcaklık artışının kütle transferini arttırdığını göstermiştir. Silikon yağı viskozitesinin değişimi makro ölçekte kütle transferini belirgin bir şekilde değiştirmemiştir. Durgun mikro

ölçekte gerçekleştirilen deneylerde sıcaklık artışının kütle transferini arttırmasının yanında DMF damlacıkları en çok en küçük viskoziteye sahip silikon yağı içinde küçülmüştür. Viskozitenin artışı ise tüm sıcaklıklarda DMF ile silikon yapı arasındaki kütle transferinin azalmasını sağlamıştır. Mikroakışkan sistem deneyleri, durgun sistemde makro ve mikro sistemde yapılan deney sonuçlarına benzer olarak, sıcaklık artışının kütle transferini arttırdığını göstermiştir. Her bir sıcaklık için silikon yağı viskozitesinin değişimi ise yine kütle transferinde belirgin bir değişikliğe sebep olmamıştır. Üç farklı deney ortamını kıyasladığımız zaman ise daha küçük ölçeklerde akış koşulları altında çözünürlüğün arttığını gösterdik. Birim zamanda birim yüzeyden gerçekleşen kütle transferinin en az makro ölçekte 25 °C'de 100 cSt'lik yağ içinde, en fazla mikroakışkan sistemde 100 °C'de yine 100 cSt'lik yağ içinde gerçekleştiğini gösterdik. Her iki ölçekte, durgun ve akış koşullarında toplamda üç deney ortamında gerçekleştirilen deney sonuçları sıcaklık artışının kütle transferini arttırdığını göstermiştir.

Keywords: İki fazlı mikroakışkan sistem, Çözünürlük, N,n-dimetilformamid (DMF), Silikon yağı, Polidimetilsilokzan (PDMS), Kütle transferi, Difüzyon, Konveksiyon, Metal organik çerçeve (MOF)

ACKNOWLEDGEMENTS

First and foremost, I would like to express my deepest gratitude to my supervisor Doç. Dr. Selis ÖNEL KAYRAN for giving guidance, motivation, and encouragement during my undergraduate and master studies. She is always passionate about continuous learning, and she integrates what she has learned into his daily life and teaches it to the people around her. Especially in the last year of my undergraduate education, these inspired me and gave me a researcher spirit. During my master's studies, she always enlightened my path and guided me to make the best decisions for my own life. I am sure that she will shed light on the path of others with his leadership.

I would like to thank and pay my regards to Prof. Dr. Burcu AKATA KURÇ, chemical engineering department in METU, Ankara for her valuable insights and for giving me to chance to work in her research lab and collaborate with her research group during the TUBİTAK project.

To my lab mates, Elif Gökçen Dilci, Buse Parlak, Anıl Hatiboğlu, and Dr. Erhan Şenlik, I thank you for your encouragement and support academically and emotionally. I am grateful for your warm friendship and great memories. It wouldn't be fun without you.

To my dearest friends, Sevde Gebeş, Özge Sevcan Hatay, Yaren Batur, İrem Korkmaz, İlayda Mutçu, Beyza TÜMER, and İlayda COŞAR, I would like to thank you for supporting me and being by my side in every situation and accepting me as I am.

To my soulmate Hasan Duman, I thank you for being you.

To my family, Sevim Korkmaz, Saim Korkmaz, and Abdulkadir Korkmaz, I am grateful to you for being with me and supporting me in every decision I make. Your presence is what makes me who I am.

The financial support provided by the Scientific and Technological Research Council of Türkiye (TUBİTAK) under grant agreement 220M002 is greatly acknowledged.

CONTENTS

Page

TABLES

FIGURES

ABBREVIATIONS

MOF	:	**M**etal **O**rganic **F**ramework
DMF	:	**D**i **M**ethyl **F**ormamide
PDMS	:	**P**oly **D**i **M**ethyl **S**iloxane
DMSO	:	**D**i **M**ethyl **S**ulf- **O**xide
PTFE	:	**P**oly **T**etra **F**luoro- **E**thylene
ITO	:	**I**ndium **T**in **O**xide
THF	:	**T**etra **H**ydro **F**uran
DMAc	:	**D**i **M**ethyl **Ac**etamide
PFCs	:	**P**er **F**luoro **M**etacrylate
DCM	:	**D**i **C**hloro **M**ethane

1. INTRODUCTION

1.1. Research Background

Nanoparticles with metal-organic framework (MOF) crystalline structures have received great attention in the energy, water treatment, pharmaceutical, and medical industries due to their extraordinary adsorption properties. MOFs have very porous structure high porosity and a high surface area-to-volume ratio. The conventional way of synthesizing nanoparticles with MOF structures is using solvothermal methods in macro-scale batch reactors [2–7]. Recently, using microfluidic systems has resulted in the synthesis of smaller and more uniform MOF nanoparticles [8]. Synthesis in microfluidics systems can be done in a single phase or in a two-phase suspension flowing in a microchannel.

Two-phase microfluidic systems, where microdroplets are formed in an oil phase and used as mini-reaction vessels, have some drawbacks during application. The nonpolar oil phase and the polar precursor solution phase may not be completely immiscible allowing for mass transfer based on the molecular structure and intermolecular forces between the liquids that are enhanced at the micro-scale and at elevated temperatures. Such diffusion of components between the two phases can affect the concentration of the precursor solution, the reaction time, and the quality of the products formed. The most frequently used solvents for the dissolution of metal salts and organic ligands in the synthesis of MOF crystalline structures are n,n-dimethylformamide (DMF), methanol, acetone, and dimethylsulfoxide (DMSO). In this study, we studied the solubility of DMF in silicone oil, polydimethylsiloxane $[-Si(CH^3)^2O-]^n)]$, which is frequently used in the formation and transportation of droplets in microchannels.

The reduction in the scale from macro to micro results in surface forces becoming more dominant over volume forces [9] such that capillarity and interface phenomena become more effective in determining the flow behavior. In the droplet-based microfluidic synthesis of MOF nanoparticles, DMF constitutes a large part of the volume of the droplet phase. The dissolution of this solvent into the silicone oil causes a reduction in the volume of

the droplets that act as a reactor and, thus, a change in the concentration of the precursor solution. Synthesis of MOF nanoparticles with the targeted properties is based on the development of recipes that involve components at specific concentrations. Maintaining a constant concentration of the precursor solution using such a recipe in droplet-based microfluidic systems is not possible due to diffusion that may occur from the droplet phase to the continuous phase. It is undesirable as it changes the conditions for synthesis and affects the quality and properties of the final product. One way to prevent the dissolution of the solvent in the precursor solution into the oil is to saturate the oil with the solvent, i.e. to add DMF into the silicon oil until the saturation point. This method does not work for flow conditions, where the convective forces between the droplet and the carrier fluid, i.e. oil, increase the saturation limit of the solvent in the oil by enhancing the transport of solvent molecules into the oil.

In this thesis study, we analyzed the decreasing the diameter and, thus, volume and surface area of the droplets and the associated mass transfer based on data from instantaneous microscopy images in the microfluidic device. To identify the effects of the droplet-based microfluidic system on the mass transport into the oil, we compared the solubility of DMF in silicone oil at macro and micro scales and under stationary and flow conditions using three different systems: 1. A stationary macro-scale system, 2. a stationary micro-scale system, and 3. a microfluidic system. We discussed the effects of convective mass diffusion by comparing the results obtained at the macro and micro scales using stationary and flow conditions and showed that solubility is enhanced under flow conditions at smaller scales.

1.2. Motivation and Objectives

In this thesis, the solubility of DMF, which is a frequently used solvent for the synthesis of MOF crystalline structures, in silicone oil, used commonly as the continuous phase in a two-phase microfluidic system, was investigated for the first time. Such a problem has not been pronounced until now in the studies of MOF synthesis employing microfluidic systems with micro reactor droplets involving precursor solutions with DMF and silicone oil

as the carrier fluid used together because the microfluidic channels in such studies consisted of opaque capillary tubes [10–13]. Such systems do not allow for the observation of the whole process starting from the formation of droplets to the formation of crystals on an optical microscope. The microfluidic system used in this study to form uniform droplets of the precursor solution in silicon oil is a transparent device made of polydimethylsiloxane (PDMS). The formation of droplets and their progress in the microchannels of the device is observed and recorded using an inverted optical microscope and an integrated fast camera. Determining the solubility limits of DMF in silicone oil, optimizing the flow conditions of the microfluidic system to determine the droplet size, and setting the initial concentration of the precursor solution in the droplet to account for the loss of DMF into the oil by dissolution will enable better control of the synthesis of MOF crystalline nanoparticles with the desired properties. Results of such solubility analyses offer researchers, who work on the synthesis of MOF nanoparticles using two phase systems, better control over formulation of precursor solution recipes. We intend to form a guide for researchers using two-phase microfluidic systems.

1.3. Outline

This thesis was organized as follows:

- Chapter 1 includes the background, motivation, and objectives underlying this study,
- Chapter 2 presents a detailed overview of MOF crystalline structures, microfluidic systems, and droplet flow in microchannels, as well as mass transfer between two phases in microfluidics,
- Chapter 3 introduces the list of materials, a detailed explanation of the systems used, fabrication of the microfluidic device, and the experimental procedures for the measurement of DMF dissolution into oil during synthesis of MOF crystalline nano particles,

- Chapter 4 lists the results with discussions based on the comparisons with the literature, and
- Chapter 5 summarizes the main conclusions and findings providing possible future ideas to expand this work.

2. LITERATURE REVIEW

2.1. Overview of Metal Organic Framework (MOF) Crystals

Metal organic framework (MOF) nanoparticles are formed by the coordination of metal ions and organic ligands. Depending on the compositions of metal ions and ligands, nanoparticles with MOFs show diverse properties, which make them attractive for use in different applications since thousands of different MOFs exist. Crystalline MOF structures have advanced adsorption capacity due to their high porosity based on an extremely high surface area to volume ratio. They can store gases, for example H_2, CH_4, and CO_2 that can be used for energy storage, gas separation, and carbon capture applications [14, 15]. Crystalline particles with MOF structures can also be used to store or hold liquids or specific materials in applications, such as controlled adsorption and release of biomolecules [16, 17], selective adsorption of toxic metals and environmental pollutants [18] depending on the intended purpose for the applications like drug delivery [19–21], controlled drug release[22], cleaning of aqueous systems [23–25], and sensing and detection [26–28].

MOFs are frequently synthesized conventionally with hydrothermal or solvothermal methods at elevated temperatures using heating in standard ovens and microwave-assisted heating. In hydrothermal or solvothermal methods, the precursor solution, which includes metal ions, organic ligands, and solvent with or without modulators is poured into a reaction vessel, such as a glass vial or autoclave, and is placed in an oven at a specific temperature for a specified synthesis time. In this method, the synthesis takes place in the reaction vessel without any mixing and takes up 2 to 5 days for the formation of high-quality crystal structures [29–31]. In the case of the microwave-assisted method, microwave irradiation is applied to the precursor solution in order to accelerate MOF formation. Microwave energy significantly reduces the synthesis time compared to the hydrothermal/solvothermal method [32]. As an alternative to these methods, microfluidic systems have become popular for the synthesis of MOF crystalline structures in recent years. Microfluidic systems are capable of providing precise control over the synthesis conditions and flow parameters enabling the formation

of high-quality MOF structures with higher crystallinity owing to higher reproducibility in shorter synthesis times [8, 33].

2.2. Dimethylformamide (DMF)

Dimethylformamide is an organic solvent in which dimethyl amide groups are attached to the carbonyl group to form the amide compound. It has a high boiling point, 153 °C, which makes it a proper choice for high-temperature solvothermal applications. DMF is a chemically stable solvent that can resist high temperatures without decomposition. DMF is a member of the class of polar aprotic solvents like acetone, acetonitrile, dimethyl sulfoxide (DMSO), dichloromethane, ethyl acetate, pyridine, and tetrahydrofuran, which can dissolve a wide range of organc and inorganic, polar and nonpolar compounds consisting of salts, acids, and bases [34]. Polar aprotic solvents have a high dielectric constant and a large dipole moment involving bonds between atoms of large difference in electronegativity.

The properties of DMF, such as the ability to dissociate salts completely and to stabilize metal nanoclusters to union with the ligands, are highly preferred in the synthesis of nanoparticles, specifically in the synthesis of MOF crystalline structures [35, 36].

DMF can be incorporated into the structure during MOF synthesis. However, this addition is usually temporary and DMF is removed from the environment at the end of the synthesis. DMF is a very stable solvent, resistant to many chemical reactions. Such features have made DMF successful in the synthesis of many MOFs and therefore frequently preferred. Changing the solvent can affect the morphology and crystal structure of the MOF structure. It may cause the production of structures with lower crystallinity or unclear morphology, agglomerate structures, and different pore sizes. In fact, the solvent used may make it difficult for metal ions to coordinate with ligands and prevent the synthesis of the MOF structure.

DMF is used in the formulations and synthesis of drugs in the pharmaceutical industry. It is used as a dispersing agent for various resins, pigments, and additives in the coatings and adhesives industry, as well as for polymers in polymerization reactions. It is used as a solvent or mobile phase for chromatographic and spectroscopic techniques in analytical chemistry.

2.3. Microfluidic Systems

Microfluidic systems have attracted attention in the recent years as tools that can be used in multidisciplinary fields for different purposes, such as chemical and biological analysis including DNA sequencing, cell sorting, and immunoassays; controlled drug delivery and drug discovery; environmental analysis and monitoring including water quality monitoring and pollutant detection; tissue engineering and synthesis of nanoparticles [11, 37, 38]. Microfluidic systems are preferred compared to conventional systems because microfluidic systems provide a safe environment for working with toxic and harmful chemicals, reduces the consumption of reagents and solvents, hence minimizing waste generation, and offers precise control of the synthesis parameters [33].

Microfluidic systems can be designed as a chip made of silicon, glass, polydimethylsiloxane (PDMS), or polymethylmethacrylate (PMMA) or with capillary tubes made of polytetrafluoroethylene (PTFE) or tygon [39]. The channel diameters are generally smaller than 900 microns [40]. The junction section where the liquids meet can be designed as X, T, or Y depending on the purpose of the study.

Microfluidic systems offer an advanced controlled environment for the synthesis of MOF crystalline structures. Synthesis parameters, such as temperature, pressure, and residence time, are controlled more precisely for the optimization of the system to produce MOF nanoparticles with intended properties. The heat and mass transfer are enhanced due to the micro distances provided by the micro channels. The advanced heat and mass transfer provide enhanced kinetics and, hence, the production of MOF crystalline structures with improved properties. Microfluidic systems offer continuous synthesis of nanoparticles in shorter synthesis times compared to conventional solvothermal batch synthesis methods. This situation ensures the production of nanocrystals with better uniformity in size [8].

Synthesis in microfluidic systems is basically grouped under two headings depending on the method, such as single-phase and two-phase microfluidic synthesis. In single-phase synthesis, the elements that form the precursor solution are given to the system from different

inlets, and the mixing of metal salt and organic ligand is provided by flowing through the microchannel. In the case of synthesis in a two-phase system, an immiscible organic phase and an aqueous phase are used to form aqueous droplets or slugs in a flowing oil phase. The mass transfer performance of slug flow over other flow regimes has been frequently examined [41–44] due to exhibiting higher stability and presenting a ratio of surface area per volume above 1000 m^2/m^3 by the domination of inertial forces [45]. A comparison [40] of mass transfer in slug flow and parallel flow in capillary channels that have small and relatively large diameters has shown that convective mass transfer becomes more effective in parallel flow exhibiting a higher mass transfer efficiency as the diameter of the channel increases, whereas mass transfer in slug flow becomes more prominent as the channel size decreases. The reason for mass transfer to become more effective in slug flow in narrower channels is that slugs get smaller and surface-to-volume ratio becomes higher and the effect of internal circulations become significant as the capillary diameter decreases [40].

For MOF synthesis studies in microfluidics, precursor solution forms the droplet phase and the formation of solid nanoparticles takes place in the droplets under specified conditions. Soybean oil is usually preferred in biological applications, while mineral oils, silicone oils, fluorinated oils, such as perfluorocarbons, and hydrocarbon oils, such as decane and dodecane, are the oils frequently used as the continuous phase in two-phase microfluidic systems.

In microfluidic systems, laminar flow exists since the channel diameters are extremely small in the order of 10^{-6} m and the liquids need to be fed to the system at smaller flow rates due to the physical and mechanical properties of the system. This results in Reynolds number generally smaller than unity and shows the dominance of viscous forces over inertial forces. Reynolds number is a dimensionless number that characterizes the flow conditions of the liquids as follows:

$$Re = \frac{l \times v \times \rho}{\mu} \tag{1}$$

where l is a characteristic length, v is the linear flow rate, ρ density, and μ viscosity of the continuous phase.

In the micro-scale, the general physics that determines the flow behaviors in microchannels is different from that of the macro scale. The inertial forces dominate the viscous forces in the macro-scale, and this offers to mix liquids easily while the opposite situation is true in the micro-scale [44]. There is always a laminar flow in microchannels and no mixing involved. In droplet flow microfluidics, the dispersed phase in the droplets flows through the channel in the continuous phase by making a continuous rotational movement [46]. Such a condition creates a mixing effect in the droplets while there is a laminar flow in the microchannels. In two-phase droplet microfluidics, homogeneous heat transfer is provided by the rotational movement of droplets. This is desired especially in studies, where heat transfer is critical, such as in solvothermal synthesis of nanoparticles.

Unsteady-state two-phase flow, where the liquid droplets flow in another immiscible liquid at an isothermal condition, is described by the fully incompressible Navier-Stokes equations as follows [47]:

$$\rho\left(\frac{\partial u}{\partial t} + u \cdot \nabla u\right) = (-\nabla p + \mu \nabla^2 u + f) \tag{2}$$

where u is the velocity field, t time, f body forces, μ viscosity, ρ is the density, and p pressure. For microfluidic systems with Reynolds numbers smaller than unity, the inertial forces are insignificant over viscous forces, such that the nonlinear terms are negligible. The Navier-Stokes equations are reduced as:

$$\rho\left(\frac{\partial u}{\partial t}\right) = (-\nabla p + \mu \nabla^2 u + f) \tag{3}$$

For the incompressible Newtonian fluids with constant density assumptions, the mass conservation due to the continuity equation is given as:

$$\nabla u = 0 \tag{4}$$

2.4. Silicone oil

Silicone oil is synthesized by repetition of silicon-oxygen chains by attaching methyl groups to silicon atoms. The existence of Si-O bonds gives unique properties to the molecule. One of them is mobility, which provides good flow properties due to the flexible rotation of the atoms around the bond. The other one is high thermal stability, which makes it a suitable choice to work at elevated temperatures without any decomposition. The Si-O bond imparts chemical inertness to the silicone oil, thus enabling it to be used in many applications. It has high electrical resistivity for use as an insulator in electrical and electronic applications. Silicone oil is also used in medical devices and drug delivery systems for biomedical applications by the contribution of Si-O bonds to make it a biocompatible material. The Si-O bond also offers hydrophobicity to the silicone oil making it a water repellent material for use in coating applications [48].

Silicone oil is a sort of methyl-terminated polymer of polydimethylsiloxane (PDMS) that is classified according to the viscosity and nature of the end groups of the polymer. The viscosity strongly depends on the length of the carbon chains and, accordingly, the molecular mass of the polymer. The physical properties of the polymer change with the viscosity until a specific value, after which they reach a limiting value even though molecular mass increases [1]. The dependence of viscosity on molecular weight is given as follows:

$$M = \frac{464(\mu_{25}^{0.825})}{2 + 0.0905(\mu_{25})^{0.555}} \tag{5}$$

where M is the molecular weight and μ_{25} is the viscosity of the silicone oil at room temperature. The viscosity of silicone oils does not depend significantly on the temperature compared to other silicone fluids and mineral oils. The relation between viscosity and temperature is given with the viscosity-temperature coefficient (VTC) as;

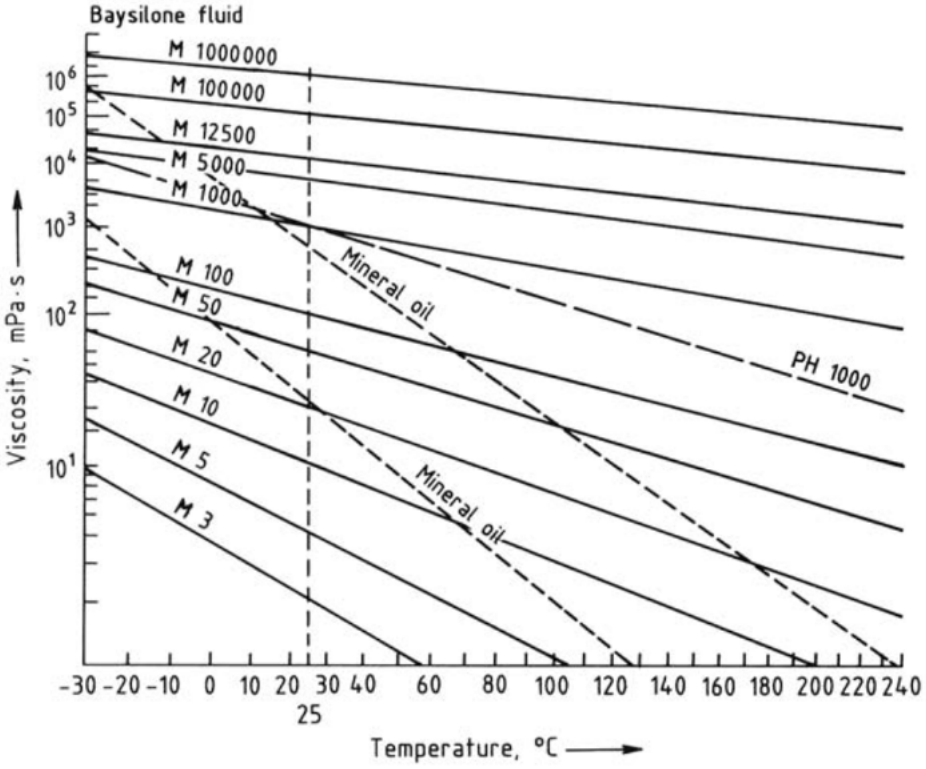

Figure 2.1 Comparing silicone oil and mineral oil due to the variation of viscosities depends on temperature [1]

$$VTC = 1 - (\frac{\mu^{99}}{\mu^{38}}) \tag{6}$$

where μ^{99}, and μ^{38} are the viscosity of silicone fluid at temperatures of 99 °C and 38 °C, respectively. VTC is equal to 0.6 for silicone fluids in the literature [1]. The temperature dependence of silicone fluids was compared with the mineral oil in Figure 3.1.

The temperature dependence on viscosity was given also for phenyl silicone fluids (PH 1000) compared to methyl silicone fluids (silicone oil) and mineral oil. It is seen that the phenyl content increases the VTC.

2.5. Transport Phenomena

In two-phase microfluidic systems, two different liquids come from two separate inlets and flow in different channels until they meet at the junction, combine and continue to flow in the jetting regime. The Rayleigh-Plateau instability occurs because of the surface tension forces between the phases and hence droplet flow appears. The size of droplets can be controlled by manipulating the flow rates of the liquids, the viscosity of the liquids, and the width of the junction. In the micro-scale, the droplets have an extremely high surface area to volume ratio, enhancing the mass transfer between the phases. The droplets produced from two immiscible liquids should be at a constant size throughout the process to maintain monodispersity, excluding any coalescence or breakup in the droplets. Even if the two fluids may be considered immiscible at a rough macroscopic glance, one may have very limited solubility in the other based on the molecular structure of the two fluids, i.e. the oil might slightly dissolve DMF causing a decrease in the volume of the DMF. Due to the nature of the droplet flow that creates an extremely high surface area to volume ratio, the mass transfer is promoted in the micro-scale and the size of the droplets might change over time.

In order to generate a droplet flow in a microfluidic system without any stimuli such as an electric field, a hydrophilic fluid such as water, organic solvents like n,n-dimethylformamide (DMF), acetone, ethanol, and tetrahydrofuran (THF), and organic-inorganic hybrid solvents like dimethyl sulfoxide (DMSO) and n,n-dimethylacetamide (DMAc) is chosen as a dispersed phase and a hydrophobic fluid such as silicone oil, mineral oil, fluorinated oils like perfluorocarbons (PFCs), chlorinated solvents like dichloromethane (DCM) and hydrocarbon solvents like hexane as a continuous phase. Such a case provides aqueous droplets in the oil. The properties of the continuous phase are extremely important for the movement and transport of droplets in the microfluidic system. The rotational and for movement of the droplets decelerates and the residence time of the droplets in the channel increases when a carrier fluid with a high-viscosity is used. In the case of a high-viscosity polymer solution used as a continuous phase, the mass transfer between the droplet phase and the continuous phase slows down due to the small mass transfer coefficients of the high-viscosity polymer

solutions [49]. Such parameters can affect the system positively or negatively depending on the purpose of the study.

The solubility of water in silicone oil has been studied by Harz et al [50]. In this study, a petri dish is covered with silicone oil, water droplets of the same size having a volume of 0.27 nl are left on the silicone oil, and another layer of silicone oil with a different viscosity is placed on the water droplets. The reason water sandwiching the droplets between the two layers of silicone oils of different viscosity was to prevent the water droplets from coalescing. Their results demonstrated the dissolution of water droplets in silicone oil. It has been found that droplet diameters decreased at an increasing rate, their volumes decreased at decreasing rate, and their cross-sectional areas decreased at a linear rate. The same experiments were repeated after the silicone oil was saturated with water. The rate of decreasing of the droplet diameters slowed down, but droplets continued to shrink. They concluded that silicone oil cannot be completely saturated with water at the micrometer scale, which is a very significant finding that should attract the attention of researchers in the microfluidics field.

Mass transfer between fluids becomes significant as the scale approaches the microns because the interfacial and viscous forces control the flow patterns while the gravitational and inertial forces become negligible [44]. Mass transfer between the phases can be desirable or undesirable in microfluidics depending on the specific purposes, applications, or processes involved.

It is desirable for chemical reaction processes, in which the reaction occurs based on the reactants encountering each other. In this case, the mass transfer promotes faster reaction kinetics and, hence, higher yield of products. Mass transfer plays a vital role in the mixing processes that provide the homogeneous mixing of different compounds rapidly in the microfluidic system. Extraction and separation studies are the other mass transfer favoring applications. Such systems are crucial for the separation of specific species between different phases. It is also desirable for chemical and biological detection as a sensor, where mass transfer of the targeted species enables accurate and sensitive detection.

Mass transfer is undesirable in the case of unfavorable species that move from one phase to another and cause possible contamination. It also renders the sample analysis challenging in that causes the sample dilution and accordingly affect the sensitivity of the analysis due to the reduced concentration of the analytes. In a two-phase microfluidic system designed for nanoparticle synthesis, the precursor solution at a specific concentration in which most of its volume is solvent forms the droplet phase while the continuous phase is a hydrophobic oil. Any mass transfer that may occur between the droplet phase and the continuous phase, changes the concentration of the precursor solution in the droplets. This is undesirable that must be managed by preventing the mass transfer between the two phases or by compensating for the mass loss as it changes the conditions for synthesis and affects the quality and properties of the final product. One way to prevent the mass transfer between the phases is to saturate the oil with the solvent. This does not work due to the flow conditions in the microfluidic systems, where the convective forces promote the mass transfer between the droplet and continuous phase and increase the saturation point due to the internal circulation in the droplets and the movement of fluids in microchannels.

The solution of unsteady mass transfer at the interface of the fluids depends on the ratio of solute diffusivity coefficients in the dispersed and continuous phases Dd/Dc, which are found using the equation derived by Sitaraman et al. [51]:

$$D_{AB} = 5.4 \times 10^{-8} [\frac{M_B^{1/2} L_B^{1/3} T}{\mu_B V_A^{0.5} L_A^{0.3}}]^{0.93} \tag{7}$$

where M_B is the molecular weight of the solvent, T is the temperature (K), μ_B is the viscosity of the solvent (cP), V_A is the molar volume of solute at boiling point in normal conditions (m^3/mol), L_A and L_B are the latent heat of vaporization of solute and solvent, respectively, at a normal boiling point (J/kg). Equation 7 is based on the correlation derived by Wilke and Chang [52]:

$$D_{AB} = 7.4 \times 10^{-8} \frac{(X M_B)^{1/2} T}{\mu_B V_A^{0.6}} \tag{8}$$

where X is the association parameter that defines the effective molecular weight of the solvent with respect to the diffusion process and is equal to 2.6 for water and 1 for nonassociated solvents.

Mass transfer resistance in the dispersed phase is attributed to the internal problem when Dd/Dc $>$ 1 while the transfer resistance in the continuous phase is assigned to the external problem when Dd/Dc $<$ 1. The transfer resistance in the dispersed and continuous phases is comparable when this ratio approaches the unity.

Mass transfer limited reactions such as nitration, hydrogenation, sulfonation, and oxidation that occur due to the transfer resistance in the dispersed phase have been employed extensively in microfluidic systems. Microfluidic systems, especially the slug flow in the small capillaries, make controlling rapid reactions possible to gain optimum yield and selectivity. The reduced path length for diffusion owing to microfluidics provides increased mass transfer efficiencies.

Burns and Ramshaw [41] used the slug flow in 380 μm wide glass microchannels for the neutralization reaction which is extremely rapid and its progress is controlled by the diffusion of the species. They used the solution of kerosene and acetic acid as an organic phase and water with KOH or NaOH as an aqueous phase. The reaction is based on the diffusion of acetic acid through the aqueous phase and neutralizes the dissolved base. In slug flow, the circulation of slugs occurs by the shear between the channel wall and the slug axis. In the presence of thin film from the organic phase, the squeezed fluid transfers the fluid from the slug ends, which enhances mixing within the slugs and provides a concentration gradient in the radial direction. They demonstrated that higher mass transfer coefficients were obtained at higher flow velocities where internal circulation and accordingly convection would be greater. This result supports the improved mass transfer across the interface by the internal circulations.

Such a neutralization reaction by the slug flow was modeled numerically in another study in a μm wide glass square microchannel with a set of partial differential equations based on computational fluid dynamics (CFD) by Harries et al. [53]. This model has postulated the

slugs as two adjacent rectangular units, which have a flat interface in the microchannel with moving walls. They demonstrated the internal circulation, which they called the internal vortex was created in both organic and aqueous slugs. Such a case offered enhanced mixing within the adjacent slugs and developed reaction rates due to refreshing acid concentration at the interface by recirculation.

Dummann et al [42] simulated the nitration reaction of a single aromatic ring using a mathematical model based on CFD with a mixture of sulfuric acid and nitric acid as the aqueous phase and an aromatic component as the organic phase. Such a study was carried out in a capillary microfluidic device similar to that of Burns and Ramshaw [41]. Their results indicated higher mass transfer efficiencies at higher flow velocities due to the internal circulations within the slugs. They also showed that decreased channel diameters led to reduced slug volumes and hence increased specific interfacial area for the mass transfer.

Kashid et al [43] developed a model considering film formation between the wall surface and slug surface. Their experimental results revealed the presence of wall film between the wall surface and the slug surface such that the effect of wall film on internal circulations was discussed using both particle image velocimetry (PIV) experiments and CFD simulations. The PIV experiments displayed the circulation patterns in the slugs with severe internal mixing which decreases the thickness of the boundary layer at the slug interface and thus improves diffusive penetration. The presence of the wall film provides that the whole surface of the slug gets involved in the mass transfer, on the contrary, only the ends of the slugs take part in the mass transfer which limits the specific surface area for the interface mass transfer. The convective mass transfer arises depending on the degree of the internal circulations whereas the interface mass transfer depends on the specific surface area between the slugs and the concentration gradient at the interface.

Suspended two-phase liquid-liquid systems in a stationary container exhibit enhanced overall mass transfer due to free convection caused by the movement and circulation of droplets under the influence of the forces of gravity and buoyancy based on density differences. Such

movements have been represented by creeping flow engaging additional mass transfer by convection.

Piarah et al [54] investigated the mass transfer of acetone between n-butyl acetate as a droplet phase and water as a continuous phase for Reynolds number was from 0.1 to 100 and Peclet number was 100. In such a study, the transfer resistance of the acetone in n-butyl acetate and water was comparable. Their results showed increasing in mass transfer with increasing Reynolds number since the increased Reynolds number promotes the convection, however, there was no significant improvement in mass transfer when Reynolds was between 0.1 and 1 due to the high Peclet number where diffusion contributed to the mass transfer compared to convection. They also repeated their calculations for the internal problem to compare that of the conjugate problem. The results demonstrated a faster decline in the concentration of acetone due to the none transfer resistance in the continuous phase. This proved the slower mass transfer in the conjugate problem than that of the internal problem.

Waheed et al [55] expressed the effect of free and forced convection on the mass transfer theoretically, numerically, and experimentally from the rising and falling droplets through the surrounding for Re$<$20. They demonstrated that free convection enhanced mass transfer over the diffusion and its effect on mass transfer was insignificant at high Reynolds numbers.

Convective mass transfer becomes important for annular and parallel flows in large capillary channels as the diameter increases resulting in larger interfacial surface area and higher mass transfer efficiencies [56]. For small capillary channels, the surface-to-volume ratio is increased by the formation of slug flow decreasing the effects of inertial forces on mass transfer and intensifying the effects of internal circulation increasing mass transfer efficiencies as the capillary diameter decreases [40]. The mass transfer performance of slug flow, where surface area-to-volume ratios of 1000 m^2/m^3 are observed, has been frequently examined over other flow regimes as they are stable and more efficient [45].

2.6. Mathematical Modelling of Mass Transfer by Molecular Diffusion

Chemical analysis of biological samples such as subcellular organelles is highly challenging due to the extremely limited amount of samples in the solution. These analyses are generally carried out by concentrating the solutes. Droplet-based suspension systems present an important area for the concentration of solutes due to providing an extremely high surface-area-to-volume ratio. As the scale approaches micrometers, the concentration of the droplets changes with the rate of the fifth power of this ratio. He et al. [57] carried out an extensive study by encapsulating the solutes in aqueous droplets that are formed in the organic phase based on the slow dissolution of water into oil. They generated aqueous droplets in the soybean oil both in a petri dish and a microchannel in contact and without contact on the surface to exhibit the effect of concentration gradient on the rate of droplet shrinkage. They described the change of the area of the water droplet with respect to time into the oil, which was considered stagnant, based on molecular diffusion as:

$$\frac{dA}{dt} = -8\pi M_w D_{w,o} \frac{Cw - Cw_{ref}}{\rho_w} = k_1 \tag{9}$$

$$A = -k_1 t + k_2 \tag{10}$$

where M_w and ρ_w refer to the molecular weight and density of the water, A is the surface area of the droplet, $D_{w,o}$ is the diffusivity of water, Cw is the concentration of water at the droplet surface, Cw_{ref} is the concentration of the water at the reference point far away from the droplet, r is the radius of the droplet and t is time. They called the 'shrinkage rate' to the k_1 where k_1 and k_2 are constants.

In another study, Bajpayee et al. [58] developed a method for the preservation of the biomaterials below the freezing point. They could control the concentration of cryoprotectant agents (CPAs) based on the solubility of water in the soybean oil by encapsulating the cell in a micro droplet containing a solution of water-glycerol into the stagnant soybean oil. The

transfer of water from the droplet phase to the oil phase increases the concentration of droplet solution enough for the vitrification of the cells by avoiding toxic injury. They integrated the diffusion model developed by He et al. [57] to obtain droplet volume, V, as a function of time, as:

$$V = (Kt + V_0^{2/3})^{3/2} \tag{11}$$

where V_0 refers to the initial volume of the droplet, and K is a constant that is given by:

$$K = -(\frac{128}{9})^{1/3}\pi^{2/3}(\frac{M_w D_{w,o} C_{sat}}{\rho_w}) \tag{12}$$

Okumuş et al. [59] studied the same application with Bajpayee et al. [58] about controlling the concentration of CPAs for the preservation of the cells in a microfluidic system. They covered the effect of convection mass transfer in addition to the molecular diffusion on the shrinkage rate of the droplets derived from Fick's Law of Diffusion and Continuity Equation, by:

$$\frac{dC_w}{dt} = \nabla \cdot (D \cdot \nabla C_w) - u \cdot \nabla C_w + Rxn \tag{13}$$

where u is the relative velocity and Rxn is the rate of creation or destruction of chemical species which is equal to zero when there is no reaction in the system.

Mass transfer in two phase systems, whether internal or conjugate, is based on the thermo-physical properties, such as solubility and surface tension, thermodynamic properties, such as temperature, pressure, and concentration, and physical properties, such as the interfacial area between the two phases that can be controlled by adjusting the geometry and size of the two phases. Keeping thermodynamic properties constant, maximization of the interfacial area and, thus, the surface area-to-volume ratio, by using smaller spherical droplets at the micro scale is possible. Subjecting spherical micro droplets to convective

forces in addition to molecular diffusion, as in droplet based microfluidic systems, will further enhance mass transfer compared to suspended systems and microfluidic systems with slug flow. Such a fact means that the dissolution rate of a substance will not be the same in a stationary or flowing and macro or micro scale system and will depend on the geometry of the interface.

3. EXPERIMENTAL METHOD

3.1. Materials

This study covers mainly the investigation of the solubility of N,N-dimethylformamide anhydrous (DMF, 99.8 %) in silicone oil (Polydimethylsiloxane, $[-Si(CH^3)^2O-]^n)]$, which were both purchased from Sigma Aldrich. The viscosity of the fluids used in the flow-focusing microfluidic device designed for droplet formation in two-phase flow has a great dependence on the flow rate. The flow rates of the two phases determine the residence time of the droplets in the microfluidic system, as well as the size of the droplets. The size of the droplets defines the interfacial area for mass transfer between the droplet and the continuous carrier phase. In order to establish the effect of viscosity on the solubility of DMF in the continuous phase, silicone oils with different viscosities, such as 100 cSt, 500 cSt, and 1000 cSt were used. The microfluidic devices were fabricated using silicone elastomer base polydimethylsiloxane (PDMS) with its curing agent (Sylgard 184, Dow Corning, Corning, NY) on optical grade, hydrolic 3 class soda lime glass microscope slides (Isolab, Istanbul). The fluids were transferred to and discharged from the microfluidic device by polytetrafluoroethylene (PTFE, Masterflex) tubes, which have a 0.305 mm inner diameter and 0.762 mm outer diameter.

3.2. Methods

The experimental procedure to investigate the solubility of DMF in silicone oil with 100 cSt, 500 cSt, and 1000 cSt viscosity was conducted under three different conditions to observe the effects of flow conditions and miniaturization on mass transfer between two phases. The three conditions can be listed as: 1. Stationary conditions in a macro scale system, 2. Stationary conditions in a suspended micro scale system, 3. Flow conditions in a microfluidic system. Each experiment was repeated 3 to 5 times until decent results were obtained.

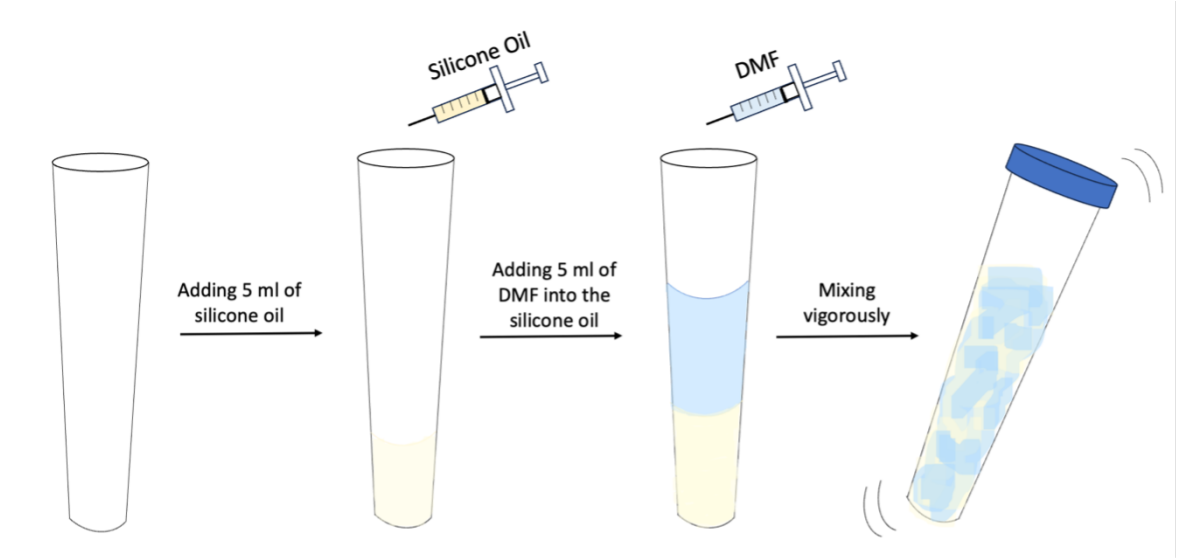

Figure 3.1 Experimental procedure for stationary macro system experiments

3.2.1. Stationary conditions in macro scale system

The macro-scale experiments were carried out in 15 ml falcon tubes as presented schematically in Figure 3.1. The initial mass of the falcon tubes containing DMF and silicone oil is listed in Table 3.1 Each tube contains 5 ml of silicon oil with a viscosity of 100 cSt, 500 cSt, and 1000 cSt. 5 ml of DMF was added into each tube containing the silicone oil and shaken vigorously for three minutes. The test tubes were left overnight for about 20 hours for complete phase separation until a meniscus between the top and bottom phases formed and remained stable. The top phase consisting of DMF was removed using a micropipette. Its mass was measured on a digital precision scale (Scaltec SBA 31). The mass loss, i.e. the difference between the initial and final mass, of DMF is presumed to be diffused into the silicone oil. This procedure was repeated at the temperatures of 25 °C, 50 °C, 75 °C and 100 °C in order to analyze the effect of temperature on mass transfer.

3.2.2. Stationary conditions in a suspended micro scale system

The stationary micro scale experiments were carried out in a specially designed stationary PDMS device with four micro wells as presented schematically in Figure 3.2. Each well

Table 3.1 The initial mass of the contents of the test tubes: DMF and silicone oil with viscosity of 100 cSt, 500 cSt, and 1000 cSt at 25 °C, 50 °C, 75 °C and 100 °C

T (°C)	Silicone oil viscosity (cSt)	Initial mass of DMF+silicone oil (g)
25	100	19.457
		19.330
		19.562
	500	19.511
		19.534
		19.362
	1000	19.512
		19.514
		19.329
50	100	19.539
		19.521
		19.497
	500	19.348
		19.494
		19.520
	1000	19.298
		19.517
		19.537
75	100	19.414
		19.465
		19.419
	500	19.427
		19.456
		19.237
	1000	19.441
		19.457
		19.209
100	100	18.873
		18.897
		18.861
	500	19.200
		18.976
		18.727
	1000	19.052
		19.050
		18.905

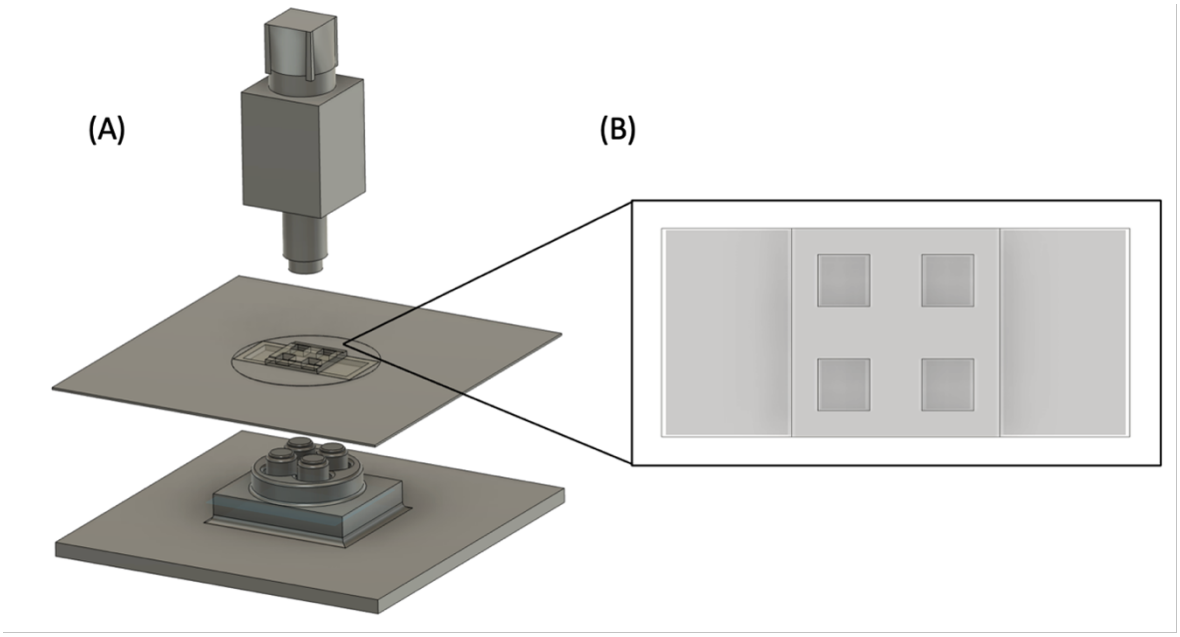

Figure 3.2 (A) Experimental setup and (B) the device designed for the stationary micro system experiments

was designed as a pool to hold the silicon oil and observe the contents on a microscope for four simultaneous experiments at the same temperature. A minimal amount of DMF was dropped in each well using the tip of a spatula. The experiment was repeated for each silicon oil with viscosities of 100 cSt, 500 cSt, and 1000 cSt. This procedure was repeated at the temperatures of 25 °C, 50 °C, 75 °C and 100 °C in order to analyze the effect of temperature on mass transfer. The DMF droplets in the silicone oil were measured, followed, and recorded using an inverted optical microscope (Olympus IX-73) and an integrated fast camera (Olympus DP73® Ultra-High Resolution Microscope Color Camera). The changes in the diameter and, thus, volume and surface area of the droplets and the associated mass transfer were analyzed based on data from instantaneous images.

3.2.3. Flow conditions in a microfluidic system

3.2.3.1. Device Fabrication The duplicate production of the microfluidic devices with a flow-focusing design was carried out as presented schematically in Figure 3.3 starting with the SU-8 molds. The molds with the desired geometry were ordered and manufactured at

Sabancı University Nanotechnology Research and Application Center (SUNUM) in Istanbul using standard photolithography methods. Such molds ensure the production of identical chips at every turn. The standard soft lithography method was used to fabricate the microfluidic devices. This method involves the mixing of PDMS and curing agent with a mass ratio of 10:1 and pouring the obtained viscous polymer solution into the SU-8 mold. In order to remove the air bubbles trapped in the polymer solution, the mold was degassed under a vacuum chamber for about an hour. After degassing, the mold was placed in the oven for curing at 80 °C for 2 hours. The cured PDMS device containing the microchannels was carefully removed from the mold using a scalpel and tweezers. Three inlet holes and an outlet hole were punched at the ends of the microchannels with a 75-gauge punch needle. One face of the PDMS device containing the microchannels and a glass microscope slide was exposed to air plasma using a plasma cleaner (Harrick Plasma Inc. PDC-32G-2 Model) providing covalent bonding when the treated sides of the PDMS and glass slide are attached to each other. The fabricated microfluidic devices were placed in the oven overnight to stabilize bonding before being used for the experiments to prevent any possible leakage.

3.2.3.2. Microfluidic Device The microfluidic device has three inlets and an outlet as shown in Figure 3.4. The silicone oil was fed to the system from the first two inlets and DMF was fed from the third inlet. The silicone oil that was fed from the second inlet is responsible for droplet formation, while the one from the first inlet is responsible for controlling the inter-droplet distance to prevent droplet coalescence. The flow-focusing microfluidic device has mainly three sections listed as the 1. x-junction, 2. auxiliary oil section, and 3. serpentine section. The droplets form at the x-junction and flow in a 200 μm wide and 100 μm high rectangular microchannel towards the auxiliary oil section. The width of the channel doubles at the auxiliary section through the end of the serpentine channel.

Experiments in the microfluidic system were conducted using an integrated system, which has an automatic computer-controlled multi-syringe system (Cetoni, NEMESYS BASE120) and an inverted microscope (Olympus IX73). A platform to hold and stabilize the microfluidic device on the microscope was designed and built using a 3D printer. The

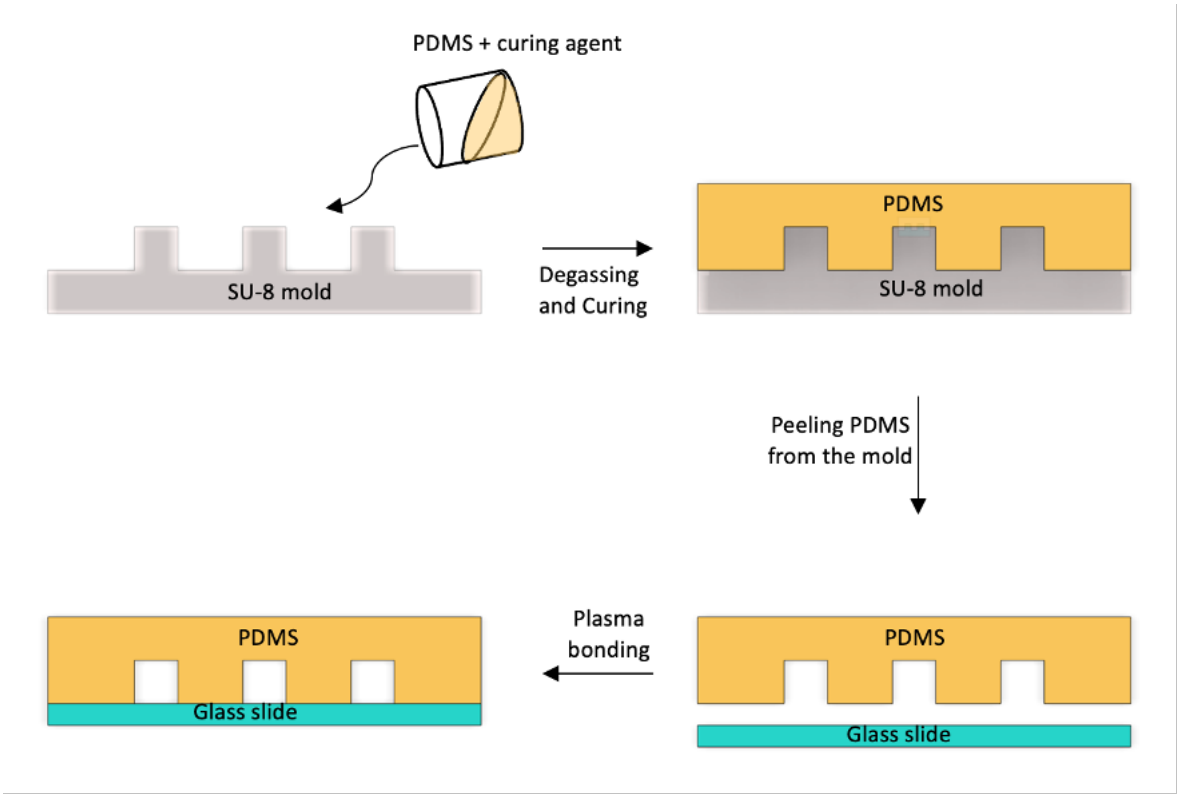

Figure 3.3 Steps of fabrication for the microfluidic device

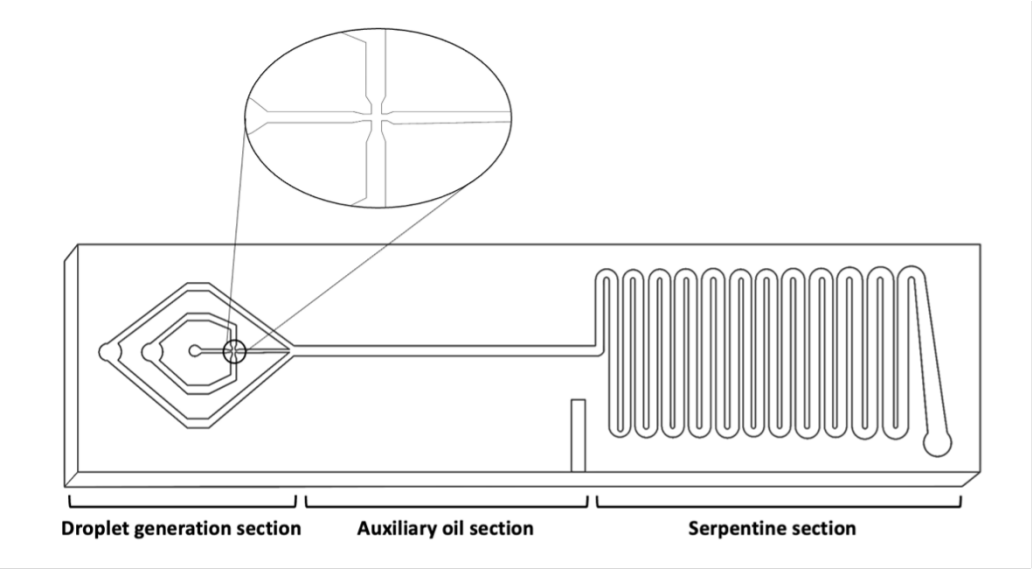

Figure 3.4 Schematic representation of the microfluidic device and its sections

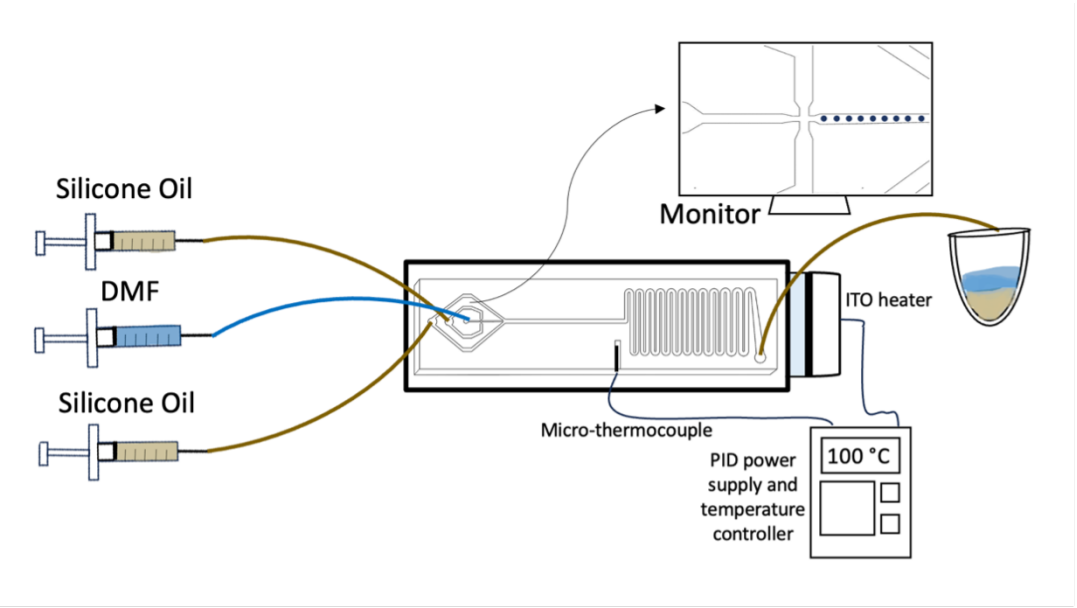

Figure 3.5 Experimental setup for a microfluidic system experiments

microfluidic device and its tubing were fixed on this platform before each experiment. The inverted microscope has image analysis features with a high-speed camera. The liquids were delivered through the microchannels by the syringe pump connected to the microfluidic device via PTFE tubing. Droplet formation in the microfluidic device was achieved by controlling the flow rates using the computer interface for the syringe pumps. Formation of the droplets and their progress in the microchannels were followed and recorded instantaneously on the computer screen using the computer interface for the microscope and fast camera. Heating was applied on the serpentine section of the microfluidic device by a transparent indium tin oxide (ITO) heater (Cell MicroControls, Norfolk, VA) for experiments at elevated temperatures as shown in the experimental set up presented in Figure 3.5. Transparency and dimensions of the ITO heaters offers them as suitable devices for use with glass and PDMS based microfluidic devices on a microscope. The ITO heater was located at the bottom of the microfluidic device below the serpentine section. The ITO heater was used together with a microthermocouple and PID temperature controller and power supply (Cell MicroControls, Norfolk, VA) to maintain the microfluidic system at a constant temperature.

We analyzed the changes in the diameter of the droplets based on data from instantaneous

images, which were taken at the x-junction and inlet, the middle, and the outlet of the serpentine section. This procedure was repeated at the temperatures of 25 °C, 50 °C, 75 °C, and 100 °C in order to analyze the effect of temperature on mass transfer.

4. RESULTS AND DISCUSSIONS

4.1. Macro Scale Experiments at Stationary Conditions

In this section, the solubility of DMF in silicone oils of various viscosities were investigated in test tubes at different temperatures. We observed that the viscosity of the continuous phase affects the size and flow rate of the droplets during synthesis of MOF nanoparticles in the two-phase microfluidic system. This directly changes the residence time of the droplets in the channel, accordingly the synthesis time, and the reactor volume. The viscosity of the dispersed phase almost remains constant as it does not change considerably based on the type of the solvents used for the complete dissociation of the salts. For the continuous phase, many oils at different viscosities are commercially available for use in microfluidics, and selection is made based on the size and material properties of the system. The selection of the oil is critical to optimize the system. In this study, the experiments were conducted with silicone oils of different viscosities, 100 cSt, 500 cSt, and 1000 cSt, in order to analyze the effect of viscosity on the solubility. The experiments were carried out at four different temperatures, 25 °C, 50 °C, 75 °C, and 100 °C, in order to investigate the effect of temperature on solubility.

The amounts of DMF that diffused into silicone oils of different viscosities at different temperatures are listed in Table 4.1 and presented graphically in Figure 4.1 The normalized volumes are obtained by dividing the final volume V of DMF by the initial volume V_0. Results show that increasing the temperature leads to a rapid decline in the volumes, which indicates an increase in diffusion of DMF into the oil as expected. This is predictable due to the exponential temperature dependence of the diffusion constant based on the Arrhenius relation. Increasing temperature increases the kinetic energy of the molecules and this promotes the motility and, hence, the collision frequency of the molecules. An increase in the kinetic energy of the molecules enhances the dissolution process.

At a macroscopic glance, DMF and silicone oil may be regarded as immiscible, which lies beneath the reason for using these fluids in microfluidic systems. However, limited dissolution occurs based on molecular diffusion, which may be enhanced by mixing or

Table 4.1 Dissolution of DMF in silicone oils of 100 cSt, 500 cSt, and 1000 cSt at 25 °C, 50 °C, 75 °C, and 100 °C in test tubes

T (°C)	Silicone oil viscosity (cSt)	Initial mass of DMF (g)	Final mass of DMF (g)	Diffused mass of DMF (g)	Diffused volume of DMF (mL)	V/V_0	Average V/V_0	Standart Deviation (V/V_0)
		4.72	4.653	0.067	0.071	0.015		
	100	4.72	4.657	0.063	0.067	0.014	0.0227	0.01400
		4.72	4.547	0.173	0.183	0.039		
		4.72	4.402	0.318	0.337	0.071		
25	**500**	4.72	4.411	0.309	0.327	0.069	0.0646	0.01009
		4.72	4.484	0.236	0.250	0.053		
		4.72	4.459	0.261	0.276	0.059		
	1000	4.72	4.529	0.191	0.202	0.043	0.0492	0.00827
		4.72	4.514	0.206	0.218	0.046		
		4.72	4.614	0.106	0.112	0.024		
	100	4.72	4.636	0.084	0.089	0.019	0.0215	0.00250
		4.72	4.622	0.098	0.104	0.022		
		4.72	4.390	0.330	0.350	0.074		
50	**500**	4.72	4.436	0.284	0.301	0.064	0.0639	0.01010
		4.72	4.480	0.240	0.254	0.054		
		4.72	4.481	0.239	0.253	0.054		
	1000	4.72	4.427	0.293	0.310	0.066	0.0561	0.00868
		4.72	4.502	0.218	0.231	0.049		
		4.72	4.470	0.250	0.265	0,056		
	100	4.72	4.535	0.185	0.196	0.042	0.0551	0.01305
		4.72	4.419	0.301	0.319	0.068		
		4.72	4.292	0.428	0.453	0.096		
75	**500**	4.72	4.342	0.378	0.400	0.085	0.0973	0.01318
		4.72	4.225	0.495	0.524	0.111		
		4.72	4.401	0.319	0.338	0.072		
	1000	4.72	4.422	0.298	0.316	0.067	0.0802	0.01913
		4.72	4.265	0.455	0.482	0.102		
		4.72	3.672	1.048	1.110	0.235		
	100	4.72	3.971	0.749	0.793	0.168	0.1974	0.03434
		4.72	3.878	0.842	0.892	0.189		
		4.72	3.970	0.750	0.794	0.168		
100	**500**	4.72	3.793	0.927	0.982	0.208	0.2129	0.04721
		4.72	3.551	1.169	1.238	0.262		
		4.72	3.799	0.921	0.976	0.207		
	1000	4.72	3.817	0.903	0.957	0.203	0.2004	0.00766
		4.72	3.865	0.855	0.906	0.192		

heating. When the two liquids are mixed, a suspension including millions of droplets forms. The molecules at the interface of the two liquids move and diffuse into the other liquid. This process takes place extremely slowly due to the limited interfacial area. The viscosity dependency of the solubility was not significantly noticeable according to mass diffusion data listed in Table 4.1 because of the insufficient amount of mass diffusion. We determined the rate of diffusion in grams of DMF per second as presented in Table 4.1 from the slope of the lines taken from the mass diffusion vs. time graphs. The diffusion rate data demonstrated increased diffusion with increased temperature. The diffusion of DMF into the silicone oil occurred nearly at the same rate at the viscosity of 100 cSt, 500 cSt, and 1000 cSt. Higher rates of diffusion were observed at all temperatures into silicone oil with the viscosity of 500 cSt. At the macro scale with stationary conditions, changing the viscosity of silicone oil did

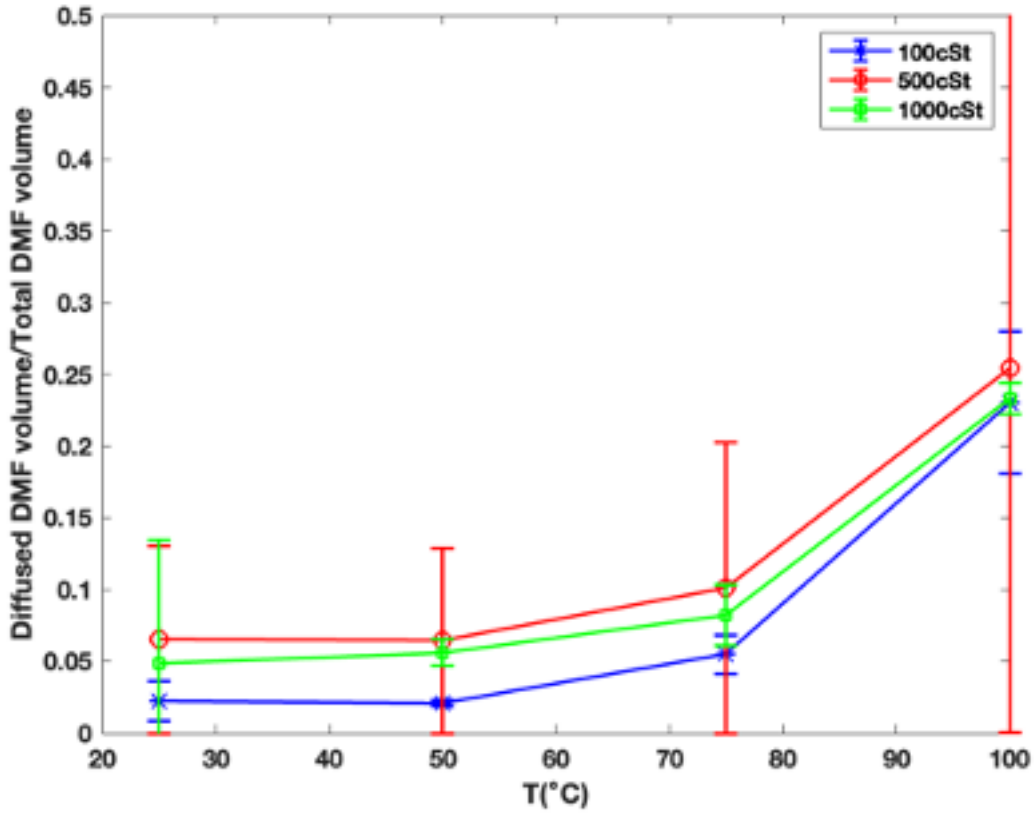

Figure 4.1 Comparison of DMF volume that diffuses into silicon oil with 100, 500, and 1000 cSt viscosity in test tubes at 25, 50, 75, and 100 °C

not significantly affect the diffusion of DMF into the oil, although, the diffusion increased with increasing the temperature from 25 °C to 100 °C.

4.2. Micro Scale Experiments at Stationary Conditions

Micro scale experiments at stationary conditions were conducted in a PDMS device which with four square micro wells. Each well is loaded with a silicone oil of the same viscosity to observe the contents on a microscope for four simultaneous experiments at the same temperature. The solubility of DMF in silicone oil with a viscosity of 100 cSt, 500 cSt, and 1000 cSt was studied into in order to analyze the effect of viscosity on solubility. The experiments were carried out at four different temperatures, 25 °C, 50 °C, 75 °C, and 100 °C, for each silicon oil in order to investigate the effect of temperature on the solubility.

Table 4.2 Rates of diffusion of DMF into silicone oil with a viscosity of 100 cSt, 500 cSt, and 1000 cSt at 25 °C, 50 °C, 75 °C, and 100 °C in test tubes

T (°C)	**Viscosity of Silicone oil (cSt)**	$\Delta Mass$ **(g)**	**Rate of total mass transfer (g/s)**	**Rate of mass transfer per volume (g/μm^3 s)**
25	**100**	0.101	1.40E-06	**3.54E-15**
	500	0.288	4.00E-06	3.50E-15
	1000	0.219	3.05E-06	3.74E-15
50	**100**	0.096	1.33E-06	7.43E-15
	500	0.285	3.95E-06	4.61E-15
	1000	0.250	3.47E-06	5.05E-15
75	**100**	0.245	3.41E-06	7.40E-15
	500	0.434	6.02E-06	5.73E-15
	1000	0.357	4.96E-06	5.73E-15
100	**100**	0.880	1.22E-05	1.72E-14
	500	0.949	1.32E-05	1.53E-14
	1000	0.893	1.24E-05	1.51E-14

Each well designed as a stationary silicone oil pool, the movement and circulation of DMF droplets, left on the top of the silicone oil, originated only under the influence of the forces of gravity and buoyancy based on density differences. Such movements have been represented by creeping flow engaging additional mass transfer by convection. The resultant additional convection based on the buoyancy forces was neglected due to the domination of molecular diffusion on mass transfer compared to convection [54]. The change in volume of the DMF droplets into the silicone oil with different viscosities, at different temperatures was listed in Table 4.3. The change in volume data showed that the maximum volume change occurred at the maximum analyzed temperature which is 100 °C and the minimum volume change occurred at the minimum analyzed temperature which is 25 °C. This is predictable due to the increased kinetic energy and promoted motility and hence collision frequency of the molecules based on the Arrhenius relation with increasing temperature. This increases the dissolution process. The data of the change of volume normalized based on the first volume of the droplets exhibited distinctly that the increasing viscosity of the silicone oil decreased the volume loss in the droplets. It was predictable because high-viscosity polymer solutions have small diffusion coefficients [49].

The temperature dependency of DMF diffusion in different viscosity silicon oils was shown graphically in Figure 4.2. For each viscosity, the minimum volume change occurred at 25

Table 4.3 The experimental results of dissolution of DMF in silicone oil with the viscosity of 100 cSt, 500 cSt, and 1000 cSt at 25 °C, 50 °C, 75 °C, and 100 °C in microwell

T (°C)	**Silicone oil viscosity (cSt)**	**Initial volume**	**Final volume**	$\Delta Volume$	$\Delta V/V_0$
25	**100**	2.14E+07	9.77E+06	1.16E+07	0.54
	500	5.88E+07	4.28E+07	1.60E+07	0.27
	1000	6.19E+07	4.78E+07	1.42E+07	0.23
50	**100**	2.71E+08	1.37E+08	1.34E+08	0.49
	500	1.94E+08	1.16E+08	7.74E+07	0.40
	1000	7.84E+07	5.95E+07	1.89E+07	0.24
75	**100**	3.71E+09	1.24E+09	2.47E+09	0.67
	500	3.74E+09	2.22E+09	1.52E+09	0.41
	1000	2.96E+09	2.08E+09	8.79E+08	0.30
100	**100**	1.17E+10	2.01E+09	9.68E+09	0.83
	500	9.73E+09	2.75E+09	6.98E+09	0.72
	1000	6.04E+09	2.81E+09	3.22E+09	0.53

°C. The shrinkage of droplets at 50 °C was generally between 25 °C and 75 °C. The highest droplet shrinkage occurred at 100 °C, and it is clearly distinguished from the others. These results demonstrated graphically the outcomes obtained from Table 4.3.

The shrinkage of the DMF droplets based on the volume change with respect to time was presented in Figure 4.3. Each graph consisted of the comparison of the volume loss of the droplets in different viscosity silicone oils, at 25 °C, 50 °C, 75 °C, and 100 °C, separately. For each temperature, the highest volume loss occurred in the silicone oil at the viscosity of 100 cSt, and the lowest shrinkage arose at the 1000 cSt silicone oil. This demonstrates graphically the results presented in Table 4.3.

The diffusion rate in grams per second is presented in Table 4.4 from the slope of the lines taken from the mass diffusion vs. time graphs. The slopes of the lines demonstrated increased diffusion with increasing temperature for each viscosity of silicone oil. The amount of diffused DMF per second was highly close to each other for the different viscosity of silicone oils at the same temperature. However, generally, the highest diffusion occurred in 100 cSt silicone oil while the lowest one took place in the 1000 cSt silicone oil. This closeness in the diffusion rates could be explained by the variation in droplet sizes. In the microwells,

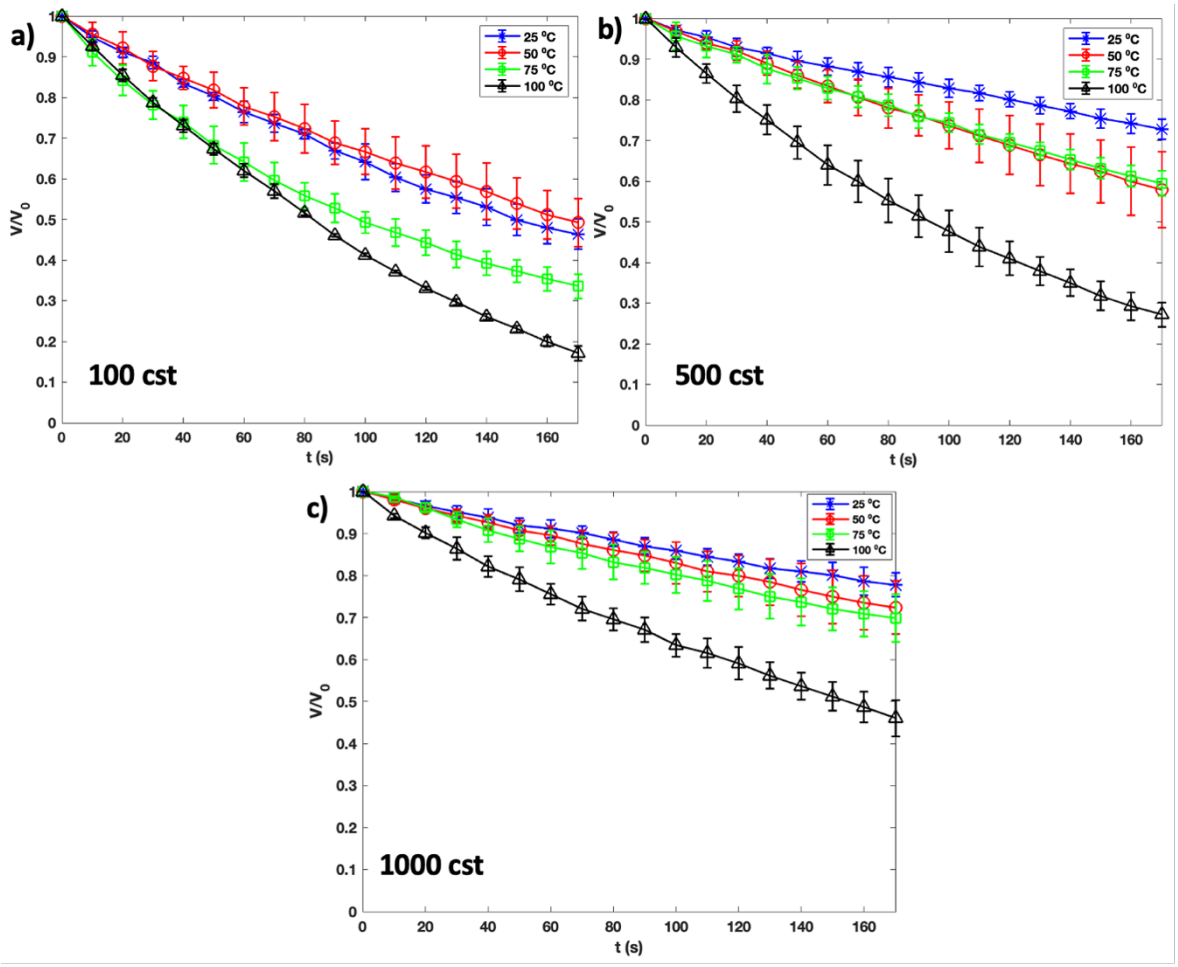

Figure 4.2 Effect of temperature at 25 °C, 50 °C, 75 °C, and 100 °C on the dissolution of DMF into silicone oil with a viscosity of a) 100 cSt, b) 500 cSt, and c) 1000 cSt in the suspended micro system in microwell

following and recording the droplets at specified droplet sizes was hard. This forced us to work in a wide range of droplet sizes between 200 microns to 1000 microns. In a micro scale with stationary conditions, increasing the viscosity of silicone oil from 100 cSt to 1000 cSt decreased the diffusion of DMF into the oil, as well as the diffusion increased with increasing temperature from 25 °C to 100 °C.

4.3. Microfluidic System Experiments at Flow Conditions

The microfluidic experiments were conducted in a PDMS-based flow-focusing device. The silicone oil flowing through two opposing channels interrupts the DMF flowing in the middle

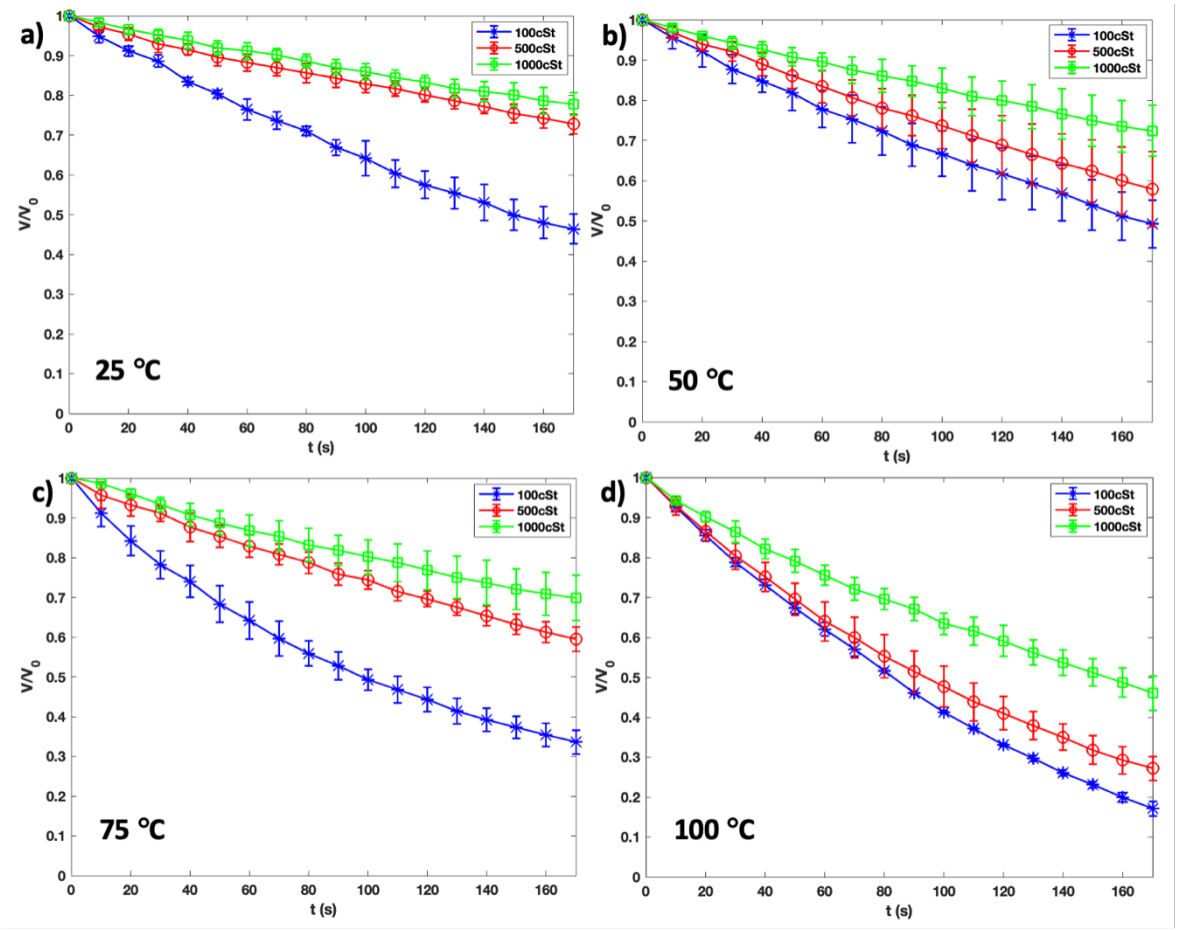

Figure 4.3 Effect of viscosity of the silicon oil at 100 cSt, 500 cSt, and 1000 cSt on the dissolution of DMF at a) 25 °C, b) 50 °C, c) 75 °C, and d) 100 °C in the suspended micro system in microwell

channel. DMF droplets formed in the x-junction of the device by Rayleigh-Plateau instability with the effect of interfacial forces between two phases. The formed droplets flow through the channel for about 413000 micrometers (0.413 m). 376000 micrometers of this path belong to the heating section at the serpentine of the device. In the microfluidic environment, flow conditions exist. Compared to stationary conditions, in the case of flow environment, there is convection mass transfer in addition to the molecular diffusion that increases the mass transfer from droplet phase to the continuous phase. Convection mass transfer occurs due to the internal circulation in the droplets and movement of the continuous phase. The movement of the continuous phase provides always feeding of the fresh fluid around the droplet. This creates always a concentration gradient between the droplet and continuous

Table 4.4 The diffusion rates of DMF in silicone oil with the viscosity of 100 cSt, 500 cSt, and 1000 cSt at 25 °C, 50 °C, 75 °C, and 100 °C in microwell

Silicone oil viscosity (cSt)	**T (°C)**	**Diffusion rate (g/s)**	**Mass transfer rate (g/μm^3 s)**
100	25	6.44E-08	3.01E-15
	50	7.42E-07	2.74E-15
	75	1.37E-05	3.70E-15
	100	5.37E-05	4.60E-15
500	25	8.87E-08	1.51E-15
	50	4.30E-07	2.22E-15
	75	8.44E-06	2.26E-15
	100	3.88E-05	3.99E-15
1000	25	7.87E-08	1.27E-15
	50	9.92E-08	1.27E-15
	75	4.88E-06	1.65E-15
	100	1.79E-05	2.96E-15

phase, and this accelerates the interface mass transfer. The flow of the continuous phase causes the droplets to rotate and move. This rotational movement creates a mixing effect that leads to an increase in the kinetic energy of the molecules. This is also promotes the mass transfer. The dissolution of DMF droplets was analyzed into the silicone oil with the viscosity of 100 cSt, 500 cSt, and 1000 cSt in order to show the effect of viscosity on mass transfer. The system was heated at four different temperatures such as 25 °C, 50 °C, 75 °C, and 100 °C to exhibit temperature dependency of mass transfer. The change in volume of the DMF droplets into the silicone oil with different viscosities, at different temperatures was listed in Table 4.5 Table 4.5 shows the volume change in DMF droplets with and without taking into consideration the first volume of the droplet. The change in volume data showed that the maximum volume change occurred at the maximum analyzed temperature which is 100 °C and the minimum volume change occurred at the minimum analyzed temperature which is 25 °C for each viscosity. This was expected due to the Arrhenius relation which explains increasing the kinetic energy and promoting motility hence increasing the collision frequency of the molecules with increasing temperature. This increases the dissolution of DMF into the oil.

Table 4.5 The experimental results of dissolution of DMF in silicone oil with the viscosity of 100 cSt, 500 cSt, and 1000 cSt at 25 °C, 50 °C, 75 °C, and 100 °C in microfluidic system

T (°C)	**Silicone oil viscosity (cSt)**	**Initial volume**	**Final volume**	$\Delta Volume$	$\Delta V/V_0$
	100	1.03E+06	5.00E+05	5.26E+05	0.51
25	500	1.05E+06	4.97E+05	5.54E+05	0.53
	1000	1.26E+06	5.73E+05	6.83E+05	0.54
	100	7.90E+05	3.35E+05	4.55E+05	0.58
50	500	1.07E+06	4.13E+05	6.61E+05	0.62
	1000	1.34E+06	4.47E+05	8.93E+05	0.67
	100	7.40E+05	1.10E+05	6.30E+05	0.85
75	500	1.05E+06	1.81E+05	8.73E+05	0.83
	1000	1.39E+06	1.66E+05	1.23E+06	0.88
	100	1.40E+06	1.48E+04	1.39E+06	0.99
100	500	1.23E+06	1.12E+04	1.22E+06	0.99
	1000	1.72E+06	6.35E+04	1.66E+06	0.96

The shrinkage of the DMF droplets into the silicone oil was analyzed graphically based on a normalized change in volume in Figure 4.4, based on a normalized change in droplet size in Figure 4.5, and based on a change in droplet size in Figure 4.6 with respect to time. Each graph compared the droplet shrinkage into the silicone oil with different viscosities at 25 °C, 50 °C, 75 °C, and 100 °C, separately. All the figures demonstrated that the increase in temperature increased the droplet shrinkage as well for each viscosity. The maximum mass loss took place at 100 °C while the minimum shrinkage occurred at 25 °C. Besides, there was no stable flow in the experiments conducted with the 100 cSt silicone oil. Especially in the serpentine section of the microfluidic device, the droplets coalesced due to the U-turns between the channels and instant instabilities with the effect of heating. For this reason, the droplets could not be followed after some time as seen in (a) picture of Figure 4.4, Figure 4.5, and Figure 4.6.

In order to analyze the viscosity dependency of mass transfer, the change in volume of DMF droplets into the silicone oil with different viscosities such as 100 cSt, 500 cSt, and 1000 cSt was presented at 25 °C, 50 °C, 75 °C, and 100 °C, separately in Figure 4.7. For each temperature, any significant relationship was not observed. The lines that represented the

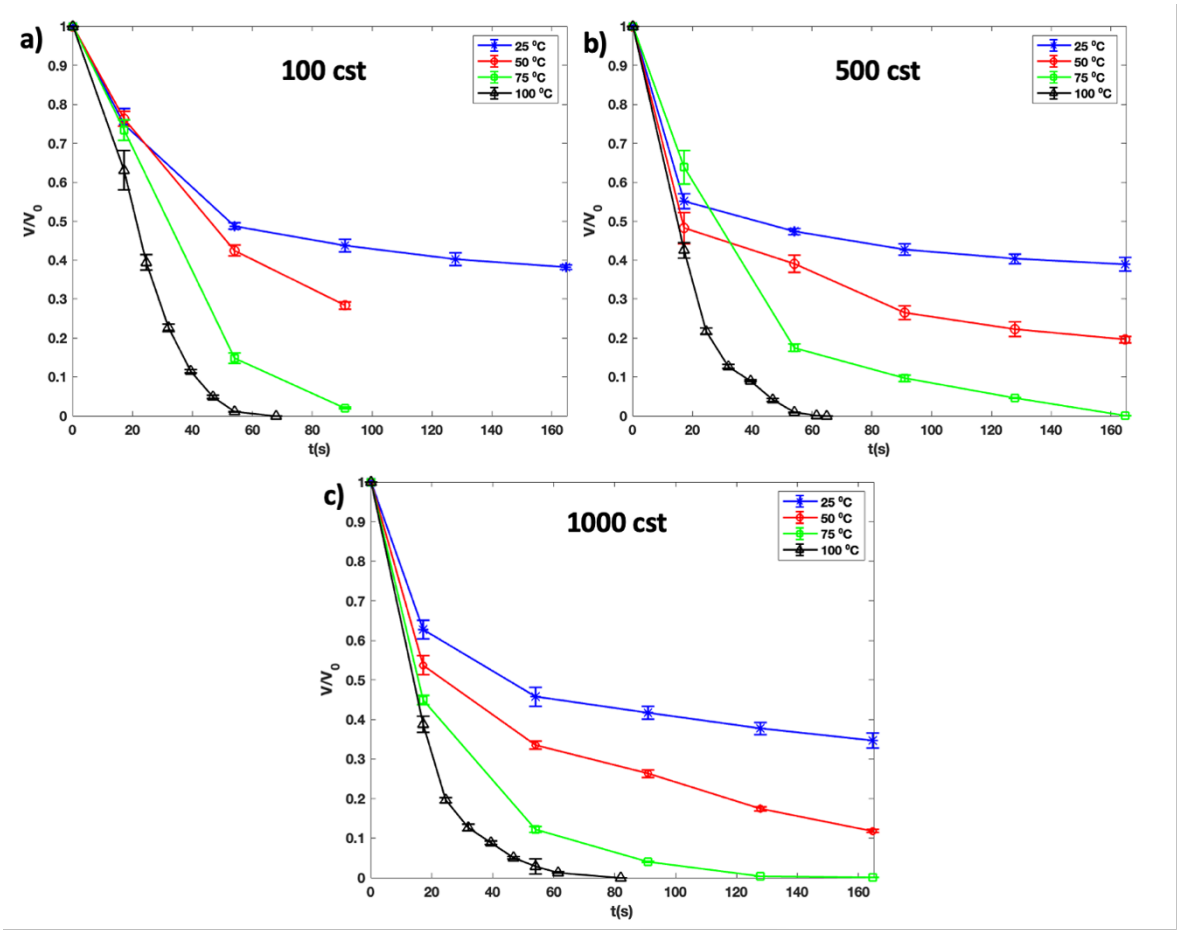

Figure 4.4 Effect of temperature at 25 °C, 50 °C, 75 °C, and 100 °C on the shrinkage of droplets based on the dissolution of DMF into silicone oil with a viscosity of a) 100 cSt, b) 500 cSt, and c) 1000 cSt in the microfluidic system based on the change in droplet volume (V/V_0)

change in volume of the droplets with respect to time had the same behavior for all viscosity of silicone oil.

The mass transfer rate in grams per second is shown in Table **??** from the slope of the lines of mass diffusion vs. time graphs. The data demonstrated the increased mass transfer rates with increasing temperature even though there is no specified behavior between the viscosity and the mass transfer rate.

In the microfluidic system, unless the experiments were conducted with the three different viscosity of silicone oils, the most stable and regular flow was evaluated with the silicone oil with a viscosity of 1000 cSt. The flow of DMF droplets into the silicone oil with a viscosity

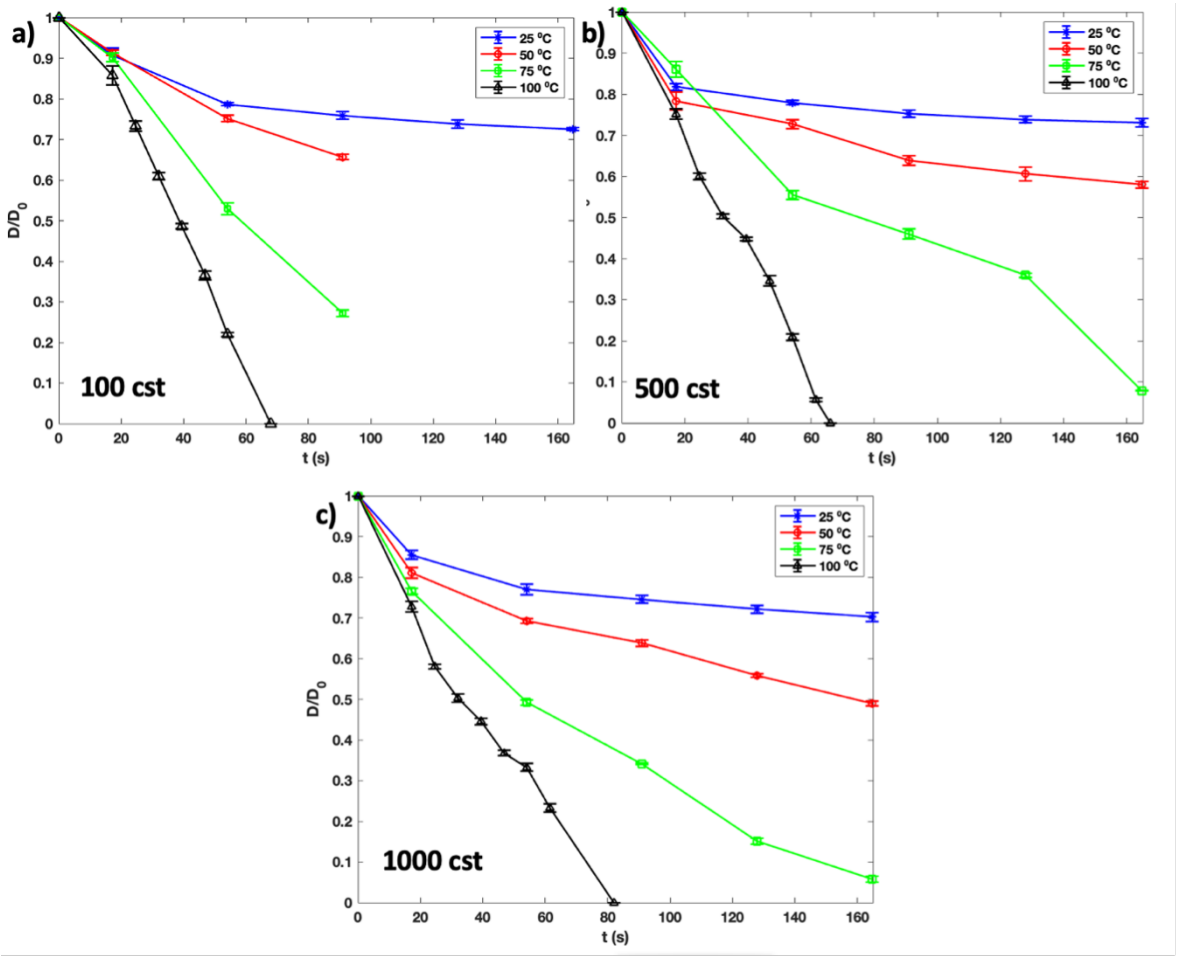

Figure 4.5 Effect of temperature at 25 °C, 50 °C, 75 °C, and 100 °C on the shrinkage of DMF droplets into silicone oil with a viscosity of a) 100 cSt, b) 500 cSt, and c) 1000 cSt in the microfluidic system based on the change in droplet size (D/D_0)

of 1000 cSt was shown in Figure 4.8 with the snapshots taken from three sections of the microfluidic device at four different temperatures such as 25 °C, 50 °C, 75 °C, and 100 °C. At the droplet formation region, the droplet sizes were nearly the same for all temperatures and flowed along the channel through the heating section. It was obviously seen that the droplet sizes were still the same before the heating region for all temperatures even though the droplets shrank a little bit until they reached the heating zone. In the heating region, the effect of temperature on droplet shrinkage was seen clearly. Increasing the temperature from 25 °C to 100 °C led to the dissolution of the DMF droplets completely.

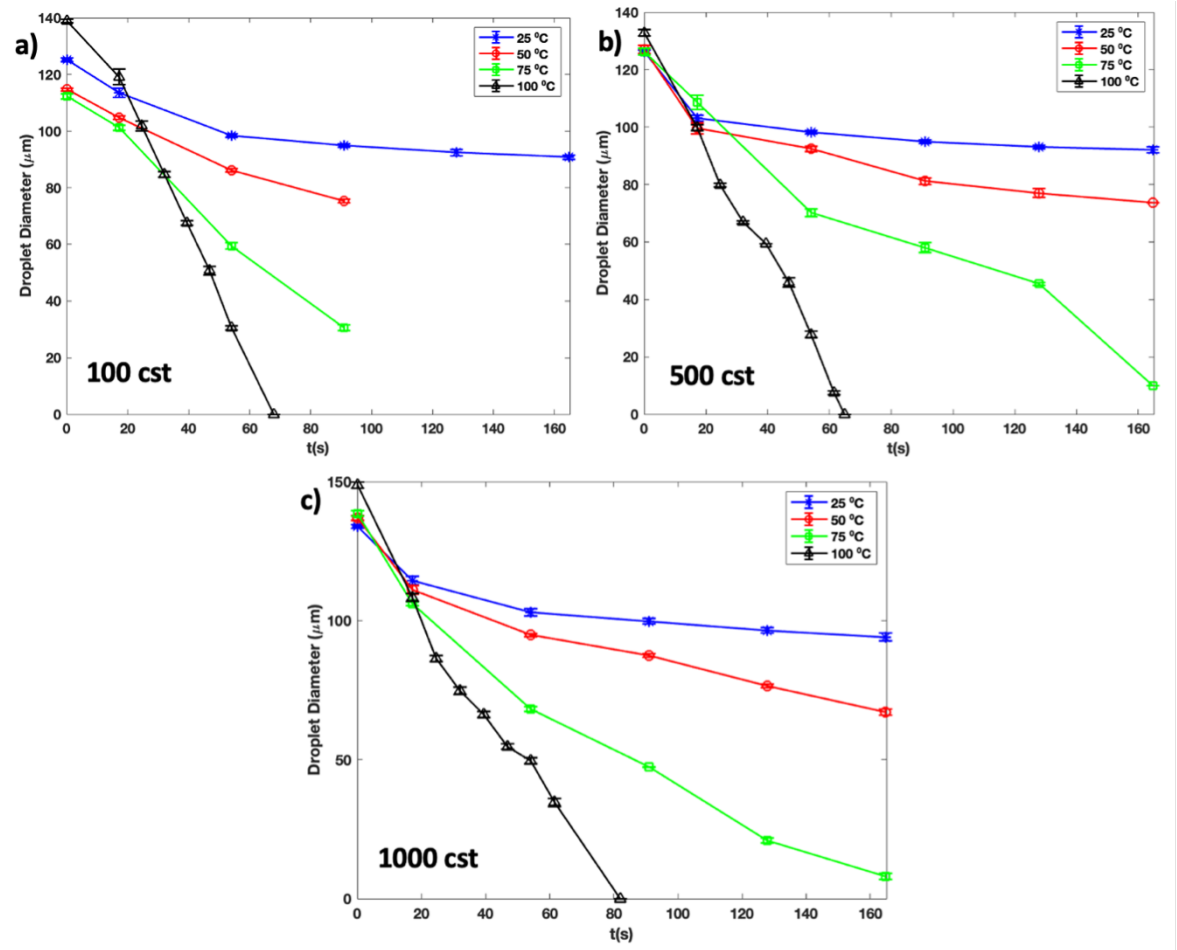

Figure 4.6 Effect of temperature at 25 °C, 50 °C, 75 °C, and 100 °C on the shrinkage of DMF droplets into silicone oil with a viscosity of a) 100 cSt, b) 500 cSt, and c) 1000 cSt in the microfluidic system based on the change in droplet size (D)

4.4. Comparison of the Dissolution of DMF into Silicon Oil under Static and Dynamic Conditions at the Micro Scale

In micro scale experiments, the stationary and fluidic conditions were examined, separately. There is only molecular diffusion between the phases while in the case of flow environment, there is convection mass transfer in addition to the molecular diffusion that increases the mass transfer from the droplet phase to the continuous phase. The comparison of the mass transfer in micro stationary and microfluidic systems is presented in Figure 4.9 for the three different viscosity of silicone oils such as 100 cSt, 500 cSt, and 1000 cSt at 25 °C, 50 °C, 75 °C, and 100 °C. For all viscosities and temperatures, the change in volume of the DMF

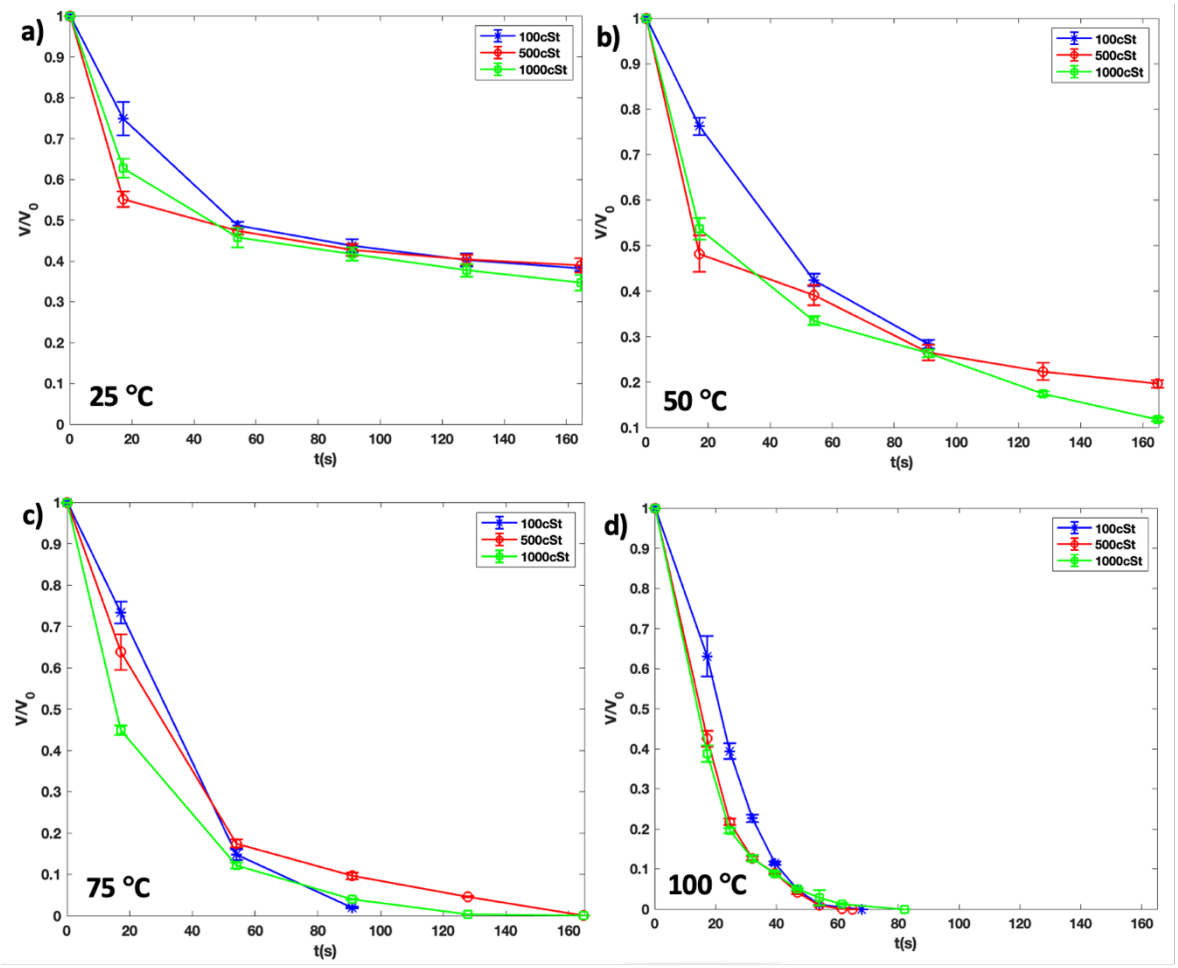

Figure 4.7 Effect of viscosity of the silicon oil at 100 cSt, 500 cSt, and 1000 cSt on the dissolution of DMF at a) 25 °C, b) 50 °C, c) 75 °C, and d) 100 °C in the microfluidic system

droplets decreased with an increasing rate in the microfluidic experiments. These results proved the effect of fluidic conditions on mass transfer due to the convective mass transfer.

In order to clarify the results evaluated from the stationary and fluidic conditions on the micro scale, the mass transfer rates in grams per second were compared for the two systems in Table 4.7. The mass transfer rates showed that the mass loss from the droplet per second was higher in micro scale stationary conditions for all viscosity of silicone oils and for all temperatures. This is not compatible with the results evaluated in Figure 4.9 which exhibited the normalized volume change of the droplet with respect to time. The reason for this inconsistency is the difference in droplet sizes from stationary and fluidic conditions. In micro stationary conditions, the droplet sizes varied between 200 microns to 1000 microns while the droplet

Table 4.6 The mass transfer rates of DMF in silicone oil with the viscosity of 100 cSt, 500 cSt, and 1000 cSt at 25 °C, 50 °C, 75 °C, and 100 °C in microfluidic system

Silicone oil viscosity (cSt)	**T (°C)**	**Mass transfer rate (g/s)**	**Mass transfer rate (g/μm^3 s)**
100	25	3.64E-09	3.54E-15
	50	5.87E-09	7.43E-15
	75	5.47E-09	7.40E-15
	100	2.42E-08	1.72E-14
500	25	3.67E-09	3.50E-15
	50	4.95E-09	4.61E-15
	75	6.03E-09	5.73E-15
	100	1.88E-08	1.53E-14
1000	25	4.70E-09	3.74E-15
	50	6.77E-09	5.05E-15
	75	7.99E-09	15.73E-15
	100	2.61E-08	1.51E-14

sizes varied between 110 microns to 150 microns in microfluidic conditions. In the bigger droplets, there was a bigger surface area per second for the mass loss. This explains the higher mass transfer rates evaluated in micro stationary systems.

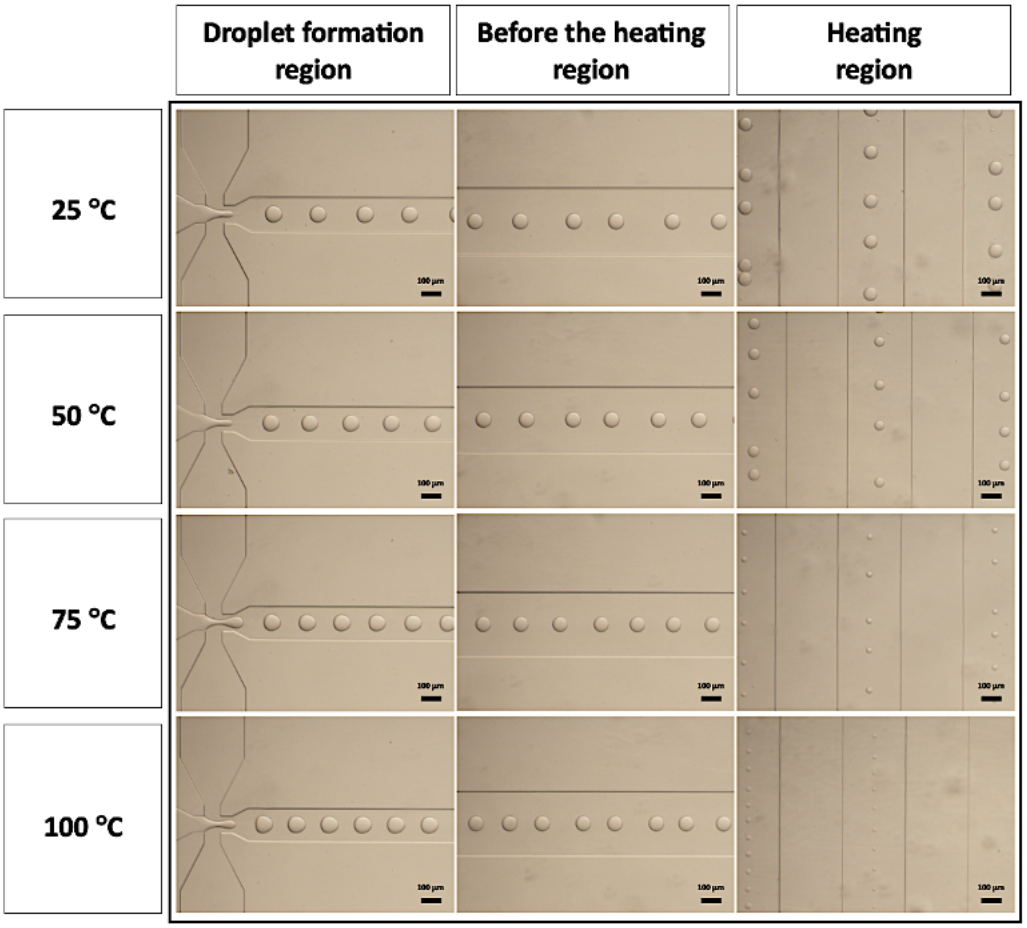

Figure 4.8 Effect of temperature on the shrinkage of DMF droplets in 1000 cSt silicon oil in the microfluidic device starting with the formation of droplets at the x-junction, during their progress in the channel before the heating region, and at the heated serpentine section

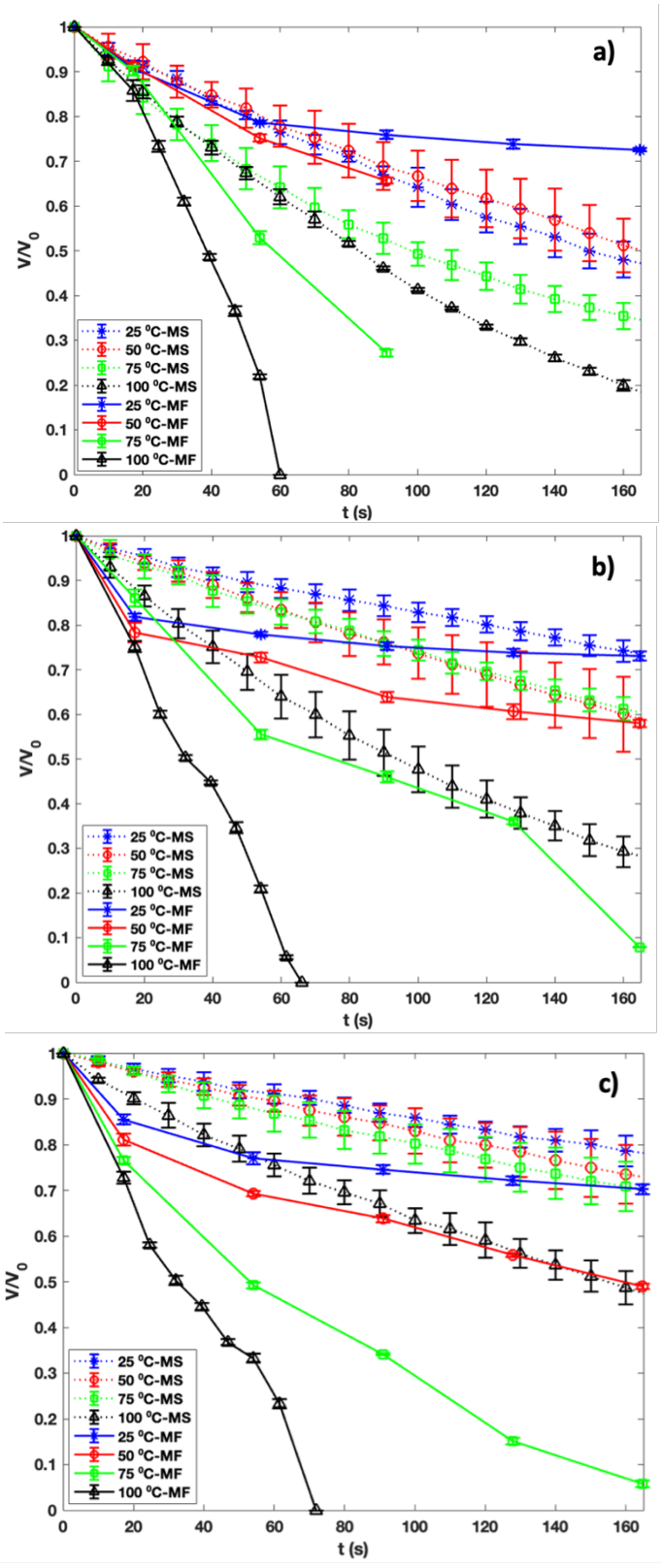

Figure 4.9 Comparison of the change in volume of DMF droplets due to dissolution into silicon oil with a viscosity of a) 100 cSt, b) 500 cSt, and c) 1000 cSt in the micro-static (MS) and microfluidic (MF) systems at 25 °C, 50 °C, 75 °C, and 100 °C

Table 4.7 Comparison of rates of mass transfer for DMF in silicone oil with a viscosity of 100 cSt, 500 cSt, and 1000 cSt at 25 °C, 50 °C, 75 °C, and 100 °C in macro stationary, micro stationary, and microfluidic systems

		Mass transfer rate (g/s)			**Mass transfer rate (g/μm^3s)**			**Mass transfer rate (g/μm^2s)**		
T (°C)	**Silicone oil viscosity (cSt)**	**Macro Stationary**	**Micro Stationary**	**Microfluidic**	**Macro Stationary**	**Micro Stationary**	**Microfluidic**	**Macro Stationary**	**Micro Stationary**	**Microfluidic**
	100	1,40E-06	6,44E-08	3,64E-09	2,81E-19	3,01E-15	3,54E-15	8,27E-18	1,79E-13	4,43E-13
25	500	4,00E-06	8,87E-08	3,67E-09	7,99E-19	1,51E-15	3,50E-15	2,35E-17	1,24E-13	4,41E-13
	1000	3,05E-06	7,87E-08	4,70E-09	6,09E-19	1,27E-15	3,74E-15	1,79E-17	1,06E-13	5,01E-13
	100	1,33E-06	7,42E-07	5,87E-09	2,67E-19	2,74E-15	7,43E-15	7,86E-18	3,71E-13	8,52E-13
50	500	3,95E-06	4,30E-07	4,95E-09	7,91E-19	2,22E-15	4,61E-15	2,33E-17	2,72E-13	5,86E-13
	1000	3,47E-06	9,92E-08	6,77E-09	6,94E-19	1,27E-15	5,05E-15	2,05E-17	1,14E-13	6,91E-13
	100	3,41E-06	1,37E-05	5,47E-09	6,81E-19	3,70E-15	7,40E-15	2,01E-17	1,20E-12	8,30E-13
75	500	6,02E-06	8,44E-06	6,03E-09	1,20E-18	2,26E-15	5,73E-15	3,55E-17	7,25E-13	7,23E-13
	1000	4,96E-06	4,88E-06	7,99E-09	9,93E-19	1,65E-15	5,73E-15	2,92E-17	4,91E-13	7,94E-13
	100	1,22E-05	5,37E-05	2,42E-08	2,44E-18	4,60E-15	1,72E-14	7,20E-17	2,16E-12	2,40E-12
100	500	1,32E-05	3,88E-05	1,88E-08	2,64E-18	3,99E-15	1,53E-14	7,76E-17	1,82E-12	2,04E-12
	1000	1,24E-05	1,79E-05	2,61E-08	2,48E-18	2,96E-15	1,51E-14	7,31E-17	1,12E-12	2,25E-12

5. CONCLUSION

In two-phase microfluidic systems designed for nanoparticle synthesis based on solvothermal methods, the droplet phase contains a precursor solution prepared by using solvents, salts, and ligands at certain concentrations, while the carrier continuous phase is an oil. The sizes of the monodispersed droplets used as capsules or reactors in two-phase microfluidic systems are expected to remain constant from the formation to the completion of the process under steady conditions unless there is any droplet coalescence or splitting. The two fluids can be assumed to be immiscible at the macro scale based on the molecular structure and physicochemical properties of the two fluids. We showed that such an assumption may cause problems with the control of the concentration of the precursor solution at the micro scale and under flow conditions. The oil might slightly dissolve DMF causing a decrease in the volume of the DMF and an increase in the concentration of the precursor solution deviating it from the set formulation. We addressed the loss of the solvent n,n-dimethylformamide (DMF) by dissolution into the carrier silicon oil in suspended systems, specifically two-phase microfluidic systems that are preferred for better control of size and structure in the synthesis of nanoparticles with metal organic framework (MOF) structures. We used silicon oils with different viscosities, 100 cSt, 500 cSt, and 1000 cSt and applied temperatures of 25 °C, 50 °C, 75 °C, and 100 °C. We showed the solubility of DMF in silicone oil at macro and micro scales and under stationary and flow conditions using three different systems: 1. A stationary macro-scale system, 2. a stationary micro-scale system, and 3. a microfluidic system. The transparent microfluidic devices made of polydimethylsiloxane (PDMS) used in this study allowed for the observation of the shrinkage of droplets on an inverted microscope. The results show that increasing temperature increases the mass transfer for the macro and micro scale and stationary and flow conditions as expected. In the stationary macro and micro experiments, the maximum amount of diffusion occurred in the silicone oil with the lowest viscosity, i.e. 100 cSt. We did not observe a specific relation between the viscosity and mass transfer in microfluidic experiments.

Mass transfer is promoted in the micro-scale depending on the chemical properties and

molecular structure of the fluids, the temperature, and the micro size of the droplets which creates an extremely high surface area-to-volume ratio, causing the droplets to shrink over time. Any mass transfer that may occur between the droplet phase and the continuous phase changes the concentration of the precursor solution in the droplets and accordingly the quality of the final product. Mass transfer between the two fluids in two-phase flow is enhanced. The surface area-to-volume ratio increases in the micro-scale causing the interfacial and viscous forces to become dominant in controlling the flow patterns, while the gravitational and inertial forces become negligible. In addition to the molecular diffusion between the droplet and the continuous phase, convection due to internal circulation in the droplets and the movement of the continuous phase with a different velocity relative to the droplet in the microchannels influences the mass transfer between the two fluids. Briefly:

(i) Mass transfer of DMF into silicon oil was not significant at the macro scale stationary conditions, which means the two liquid phases may be regarded as immiscible at the macro scale.

(ii) Mass transfer became significant as the scale approached the micron level, i.e. molecular diffusion between the droplet and continuous phase is enhanced due to surface forces.

(iii) In microfluidic conditions, mass transfer increased due to convective mass transport based on fluid flow in the microchannel and internal circulation of droplets. This means that the two phases cannot be regarded as immiscible and diffusion of DMF into the oil must be accounted for.

(iv) Silicon oil with a lower viscosity, i.e. 100 cSt followed by 500 cSt and 1000 cSt, allowed for larger amount of mass transfer. Silicon oil with the viscosity of 1000 cSt was found to be most suitable for microfluidic studies due to minimal diffusion of DMF allowed.

(v) The rate of dissolution of DMF per surface area was the lowest for the 100 cSt oil in the macro stationary system with $8.27x10^{-18}$ g/μm^2s at the 25 °C the highest for the

100 cSt oil in the microfluidic system with $2.40x10^{-12}$ g/μm^2s at 100 °C, i.e. about 10^6 times higher than that for the stationary macro scale and microfluidic systems.

(vi) Increase in temperature from 25, 50, 75, to 100 °C resulted in enhanced diffusion of DMF into the oil in all cases as expected.

The enhanced dissolution at the micro-scale could be desirable or undesirable depending on the purpose of the study in microfluidics. In this study, we did not investigate the effects of solely convective forces in the microfluidic system. Such a study was conducted by Okumuş et al. [59] using mathematical models. An extension of this study could involve empirical and theoretical analysis of no flow and various flow rates on the rate of dissolution of DMF into a silicon oil of 1000 cSt viscosity, which was shown to be the oil with minimal dissolving capacity for DMF.

REFERENCES

[1] Hans-Heinrich Moretto, Manfred Schulze, and Gebhard Wagner. Silicones. *Ullmann's encyclopedia of industrial chemistry*, **2000**.

[2] Norbert Stock and Shyam Biswas. Synthesis of metal-organic frameworks (mofs): routes to various mof topologies, morphologies, and composites. *Chemical reviews*, 112(2):933–969, **2012**.

[3] Takaaki Tsuruoka, Shuhei Furukawa, Yohei Takashima, Kaname Yoshida, Seiji Isoda, and Susumu Kitagawa. Nanoporous nanorods fabricated by coordination modulation and oriented attachment growth. *Angewandte Chemie*, 121(26):4833–4837, **2009**.

[4] Jianhao Qiu, Yi Feng, Xiongfei Zhang, Mingmin Jia, and Jianfeng Yao. Acid-promoted synthesis of uio-66 for highly selective adsorption of anionic dyes: Adsorption performance and mechanisms. *Journal of colloid and interface science*, 499:151–158, **2017**.

[5] Guang Lu, Chenlong Cui, Weina Zhang, Yayuan Liu, and Fengwei Huo. Synthesis and self-assembly of monodispersed metal-organic framework microcrystals. *Chemistry–An Asian Journal*, 8(1):69–72, **2013**.

[6] Panpan Niu, Ningyue Lu, Jiaojiao Liu, Huanhuan Jia, Fan Zhou, Binbin Fan, and Ruifeng Li. Water-induced synthesis of hierarchical zr-based mofs with enhanced adsorption capacity and catalytic activity. *Microporous and Mesoporous Materials*, 281:92–100, **2019**.

[7] Florence Ragon, Patricia Horcajada, Hubert Chevreau, Young Kyu Hwang, U-Hwang Lee, Stuart R Miller, Thomas Devic, Jong-San Chang, and Christian Serre. In situ energy-dispersive x-ray diffraction for the synthesis optimization and scale-up of the porous zirconium terephthalate uio-66. *Inorganic chemistry*, 53(5):2491–2500, **2014**.

[8] Samar Damiati, Uday B Kompella, Safa A Damiati, and Rimantas Kodzius. Microfluidic devices for drug delivery systems and drug screening. *Genes*, 9(2):103, **2018**.

[9] Pantcho Stoyanov and Richard R Chromik. Scaling effects on materials tribology: from macro to micro scale. *Materials*, 10(5):550, **2017**.

[10] Marco Faustini, Jun Kim, Guan-Young Jeong, Jin Yeong Kim, Hoi Ri Moon, Wha-Seung Ahn, and Dong-Pyo Kim. Microfluidic approach toward continuous and ultrafast synthesis of metal–organic framework crystals and hetero structures in confined microdroplets. *Journal of the American Chemical Society*, 135(39):14619–14626, **2013**.

[11] Lorena Paseta, Beatriz Seoane, Daniel Julve, Víctor Sebastián, Carlos Téllez, and Joaquín Coronas. Accelerating the controlled synthesis of metal–organic frameworks by a microfluidic approach: a nanoliter continuous reactor. *ACS Applied Materials & Interfaces*, 5(19):9405–9410, **2013**.

[12] Oleksii Kolmykov, Jean-Marc Commenge, Halima Alem, Emilien Girot, Kevin Mozet, Ghouti Medjahdi, and Raphaël Schneider. Microfluidic reactors for the size-controlled synthesis of zif-8 crystals in aqueous phase. *Materials & Design*, 122:31–41, **2017**.

[13] Angelos Polyzoidis, T Altenburg, M Schwarzer, Stefan Löbbecke, and S Kaskel. Continuous microreactor synthesis of zif-8 with high space–time-yield and tunable particle size. *Chemical Engineering Journal*, 283:971–977, **2016**.

[14] Alexander Schoedel, Zhe Ji, and Omar M Yaghi. The role of metal–organic frameworks in a carbon-neutral energy cycle. *Nature Energy*, 1(4):1–13, **2016**.

[15] Sibo Wang and Xinchen Wang. Imidazolium ionic liquids, imidazolylidene heterocyclic carbenes, and zeolitic imidazolate frameworks for co2 capture and photochemical reduction. *Angewandte Chemie International Edition*, 55(7):2308–2320, **2016**.

[16] Patricia Horcajada, Ruxandra Gref, Tarek Baati, Phoebe K Allan, Guillaume Maurin, Patrick Couvreur, Gérard Férey, Russell E Morris, and Christian Serre. Metal–organic frameworks in biomedicine. *Chemical reviews*, 112(2):1232–1268, **2012**.

[17] Chunbai He, Demin Liu, and Wenbin Lin. Nanomedicine applications of hybrid nanomaterials built from metal–ligand coordination bonds: nanoscale metal–organic frameworks and nanoscale coordination polymers. *Chemical reviews*, 115(19):11079–11108, **2015**.

[18] Jiewei Liu, Lianfen Chen, Hao Cui, Jianyong Zhang, Li Zhang, and Cheng-Yong Su. Applications of metal–organic frameworks in heterogeneous supramolecular catalysis. *Chemical Society Reviews*, 43(16):6011–6061, **2014**.

[19] Bader M Jarai, Zachary Stillman, Lucas Attia, Gerald E Decker, Eric D Bloch, and Catherine A Fromen. Evaluating uio-66 metal–organic framework nanoparticles as acid-sensitive carriers for pulmonary drug delivery applications. *ACS applied materials & interfaces*, 12(35):38989–39004, **2020**.

[20] Johannes WM Osterrieth and David Fairen-Jimenez. Metal–organic framework composites for theragnostics and drug delivery applications. *Biotechnology Journal*, 16(2):2000005, **2021**.

[21] Jian Cao, Xuejiao Li, and Hongqi Tian. Metal-organic framework (mof)-based drug delivery. *Current medicinal chemistry*, 27(35):5949–5969, **2020**.

[22] Vladimir R Cherkasov, Elizaveta N Mochalova, Andrey V Babenyshev, Julian M Rozenberg, Ilya L Sokolov, and Maxim P Nikitin. Antibody-directed metal-organic framework nanoparticles for targeted drug delivery. *Acta Biomaterialia*, 103:223–236, **2020**.

[23] Huaiyin Chen, Fangfang Wang, Huizhou Fan, Ruoyu Hong, and Weihua Li. Construction of mof-based superhydrophobic composite coating with excellent abrasion resistance and durability for self-cleaning, corrosion resistance,

anti-icing, and loading-increasing research. *Chemical Engineering Journal*, 408:127343, **2021**.

[24] Ke Li, Nicholas Miwornunyuie, Lei Chen, Huang Jingyu, Paulette Serwaa Amaniampong, Desmond Ato Koomson, David Ewusi-Mensah, Wencong Xue, Guang Li, and Hai Lu. Sustainable application of zif-8 for heavy-metal removal in aqueous solutions. *Sustainability*, 13(2):984, **2021**.

[25] Farid Mzee Mpatani, Aaron Albert Aryee, Alexander Nti Kani, Runping Han, Zhaohui Li, Evans Dovi, and Lingbo Qu. A review of treatment techniques applied for selective removal of emerging pollutant-trimethoprim from aqueous systems. *Journal of Cleaner Production*, 308:127359, **2021**.

[26] S Homayoonnia and S Zeinali. Design and fabrication of capacitive nanosensor based on mof nanoparticles as sensing layer for vocs detection. *Sensors and Actuators B: Chemical*, 237:776–786, **2016**.

[27] Miguel A Andrés, Mani Teja Vijjapu, Sandeep G Surya, Osama Shekhah, Khaled Nabil Salama, Christian Serre, Mohamed Eddaoudi, Olivier Roubeau, and Ignacio Gascón. Methanol and humidity capacitive sensors based on thin films of mof nanoparticles. *ACS applied materials & interfaces*, 12(3):4155–4162, **2020**.

[28] Wei Shi, Mengqi He, Weitao Li, Xing Wei, Brian Bui, Mingli Chen, and Wei Chen. Cu-based metal–organic framework nanoparticles for sensing cr (vi) ions. *ACS Applied Nano Materials*, 4(1):802–810, **2021**.

[29] Bing He, Qichong Zhang, Ping Man, Zhenyu Zhou, Chaowei Li, Qiulong Li, Liyan Xie, Xiaona Wang, Huan Pang, and Yagang Yao. Self-sacrificed synthesis of conductive vanadium-based metal–organic framework nanowire-bundle arrays as binder-free cathodes for high-rate and high-energy-density wearable zn-ion batteries. *Nano Energy*, 64:103935, **2019**.

[30] Jie Yang, Hailin Tian, Yang Li, He Li, Shuo Li, Haitao Yang, Meng Ding, Xiaonan Wang, and Po-Yen Chen. Eco-friendly synthesis of vanadium metal-organic frameworks from gasification waste for wearable zn-ion batteries. *Energy Storage Materials*, 53:352–362, **2022**.

[31] Mahmoud Y Zorainy, Mohamed Sheashea, Serge Kaliaguine, Mohamed Gobara, and Daria C Boffito. Facile solvothermal synthesis of a mil-47 (v) metal–organic framework for a high-performance epoxy/mof coating with improved anticorrosion properties. *RSC advances*, 12(15):9008–9022, **2022**.

[32] Kalya Jagannatha Rao, Bala Vaidhyanathan, Munia Ganguli, and PA Ramakrishnan. Synthesis of inorganic solids using microwaves. *Chemistry of materials*, 11(4):882–895, **1999**.

[33] Holger Bolze, Peer Erfle, Juliane Riewe, Heike Bunjes, Andreas Dietzel, and Thomas P Burg. A microfluidic split-flow technology for product characterization in continuous low-volume nanoparticle synthesis. *Micromachines*, 10(3):179, **2019**.

[34] D Stoye. Ullmann's encyclopedia of industrial chemistry: Solvents, **2000**.

[35] Majid M Heravi, Mahdieh Ghavidel, and Leyla Mohammadkhani. Beyond a solvent: triple roles of dimethylformamide in organic chemistry. *RSC advances*, 8(49):27832–27862, **2018**.

[36] Hussein Rasool Abid, Jin Shang, Ha-Ming Ang, and Shaobin Wang. Amino-functionalized zr-mof nanoparticles for adsorption of co2 and ch4. *International Journal of Smart and Nano Materials*, 4(1):72–82, **2013**.

[37] Gaofei Hu, Lili Yang, Yina Li, and Leyu Wang. Continuous and scalable fabrication of stable and biocompatible mof@ sio 2 nanoparticles for drug loading. *Journal of Materials Chemistry B*, 6(47):7936–7942, **2018**.

[38] Jie Shen, Muhammad Shafiq, Ming Ma, and Hangrong Chen. Synthesis and surface engineering of inorganic nanomaterials based on microfluidic technology. *Nanomaterials*, 10(6):1177, **2020**.

[39] J. Jovanovic. *Liquid-liquid microreactors for phase transfer catalysis*. Phd thesis 1 (research tu/e / graduation tu/e), Chemical Engineering and Chemistry, **2011**. doi:10.6100/IR719772.

[40] Rahul Antony, MS Giri Nandagopal, Nidhin Sreekumar, S Rangabhashiyam, and N Selvaraju. Liquid-liquid slug flow in a microchannel reactor and its mass transfer properties-a review. *Bulletin of Chemical Reaction Engineering & Catalysis*, 9(3):207, **2014**.

[41] JR Burns and C Ramshaw. The intensification of rapid reactions in multiphase systems using slug flow in capillaries. *Lab on a Chip*, 1(1):10–15, **2001**.

[42] Gerrit Dummann, Ulrich Quittmann, Lothar Gröschel, David W Agar, Otto Wörz, and Konrad Morgenschweis. The capillary-microreactor: a new reactor concept for the intensification of heat and mass transfer in liquid–liquid reactions. *Catalysis today*, 79:433–439, **2003**.

[43] Madhvanand N Kashid, I Gerlach, S Goetz, J Franzke, JF Acker, F Platte, David W Agar, and Stefan Turek. Internal circulation within the liquid slugs of a liquid- liquid slug-flow capillary microreactor. *Industrial & engineering chemistry research*, 44(14):5003–5010, **2005**.

[44] Anne-Laure Dessimoz, Laurent Cavin, Albert Renken, and Lioubov Kiwi-Minsker. Liquid–liquid two-phase flow patterns and mass transfer characteristics in rectangular glass microreactors. *Chemical Engineering Science*, 63(16):4035–4044, **2008**.

[45] Jovan Jovanović, Evgeny V Rebrov, TA Nijhuis, Volker Hessel, and Jaap C Schouten. Phase-transfer catalysis in segmented flow in a microchannel: fluidic

control of selectivity and productivity. *Industrial & Engineering Chemistry Research*, 49(6):2681–2687, **2010**.

[46] Chunyang Wei, Chengzhuang Yu, Shanshan Li, Feng Pan, Tiejun Li, Zichao Wang, and Junwei Li. Rapid microfluidic mixing method based on droplet rotation due to pdms deformation. *Micromachines*, 12(8):901, **2021**.

[47] CJ Geankoplis. Transport processes and separation. *Process Principles, Prentice Hall NJ*, **2003**.

[48] JA Brydson. Silicones and other heat resisting polymers. *Plastics Materials*, 6:792–818, **1999**.

[49] Steffen Hardt and Thomas Hahn. Microfluidics with aqueous two-phase systems. *Lab on a Chip*, 12(3):434–442, **2012**.

[50] M Harz and M Knoche. Droplet sizing using silicone oils. *Crop Protection*, 20(6):489–498, **2001**.

[51] Ramalingam Sitaraman, SH Ibrahim, and NR Kuloor. A generalized equation for diffusion in liquids. *Journal of Chemical and Engineering Data*, 8(2):198–201, **1963**.

[52] CR Wilke and Pin Chang. Correlation of diffusion coefficients in dilute solutions. *AIChE journal*, 1(2):264–270, **1955**.

[53] N Harries, JR Burns, David Anthony Barrow, and C Ramshaw. A numerical model for segmented flow in a microreactor. *International journal of heat and mass transfer*, 46(17):3313–3322, **2003**.

[54] WH Piarah, A Paschedag, and M Kraume. Numerican simulation of mass transfer between a single drop and an ambient flow. *American Institute of Chemical Engineers. AIChE Journal*, 47(7):1701, **2001**.

[55] M Adekojo Waheed, Martin Henschke, and Andreas Pfennig. Mass transfer by free and forced convection from single spherical liquid drops. *International Journal of Heat and Mass Transfer*, 45(22):4507–4514, **2002**.

[56] Xu Bin Zhang, Dan Chen, Yan Wang, and Wang Feng Cai. Liquid-liquid two-phase flow patterns and mass transfer characteristics in a circular microchannel. *Advanced Materials Research*, 482:89–94, **2012**.

[57] Mingyan He, Chenhang Sun, and Daniel T Chiu. Concentrating solutes and nanoparticles within individual aqueous microdroplets. *Analytical chemistry*, 76(5):1222–1227, **2004**.

[58] Anurag Bajpayee, Jon F Edd, Anthony Chang, and Mehmet Toner. Concentration of glycerol in aqueous microdroplets by selective removal of water. *Analytical chemistry*, 82(4):1288–1291, **2010**.

[59] Ufuk Okumus. *Examination And Mathematical Modelling Of Shrinkage Rate Of Uniform Droplets In A Microfluidic System Designed For Biopreservation*. Ph.D. thesis, Hacettepe University, **2015**.